



Elettra Sincrotrone Trieste



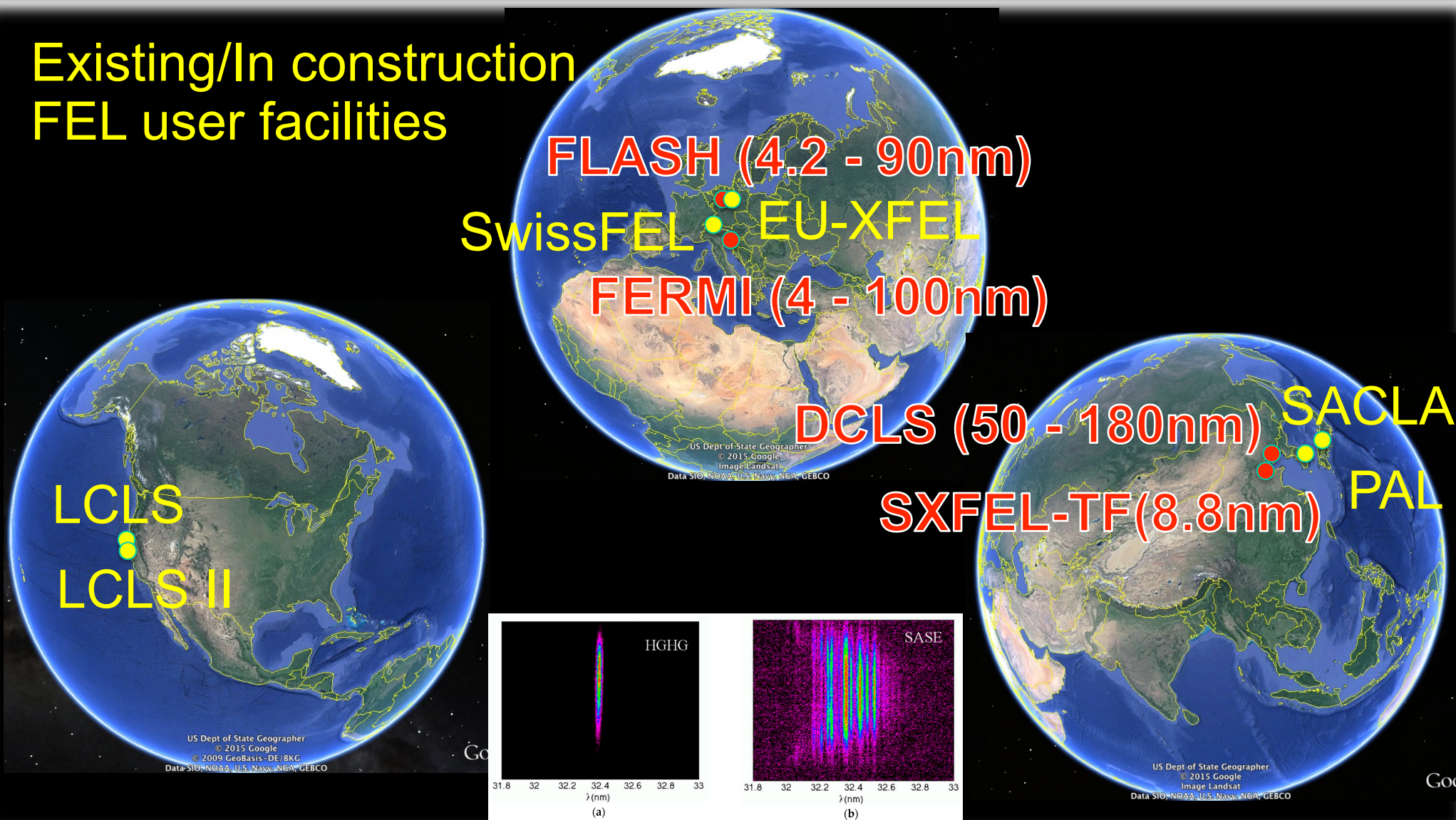
# Photon beam transport and diagnostics systems at an EUV FEL facility: general considerations, and specific challenges, solutions and developments at the FERMI seeded FEL

**Marco Zangrando**  
On behalf of the FERMI team

**FEL 2017**  
20<sup>th</sup> - 25<sup>th</sup> August, 2017  
Santa Fe Convention Center, Santa Fe, NM USA  
38<sup>th</sup> International Free Electron Laser Conference

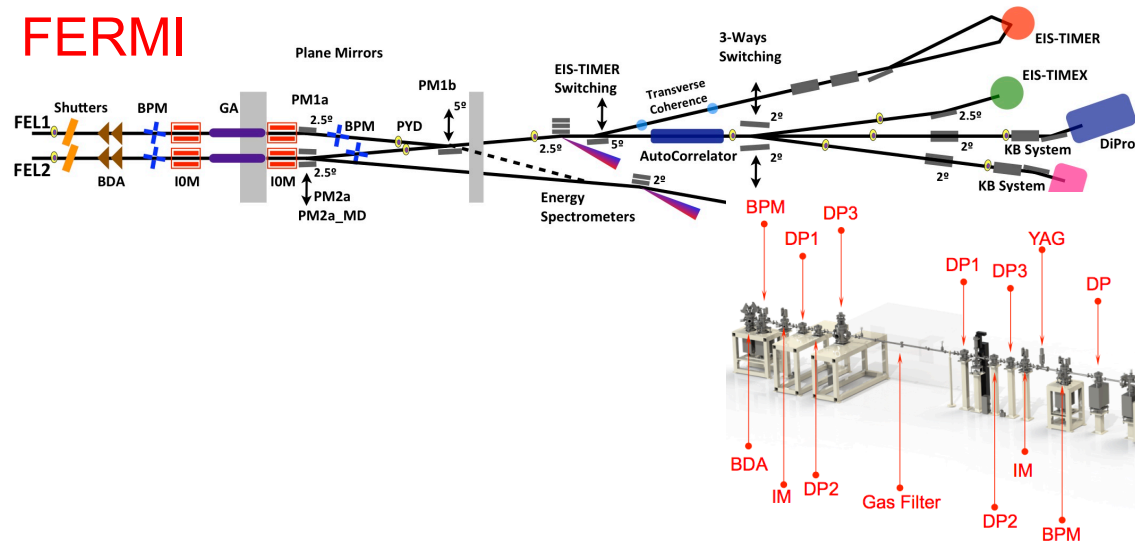


## Existing/In construction FEL user facilities

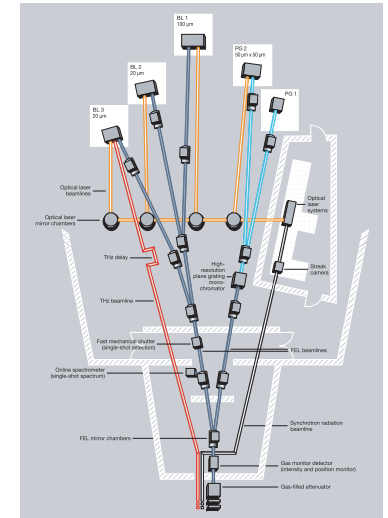




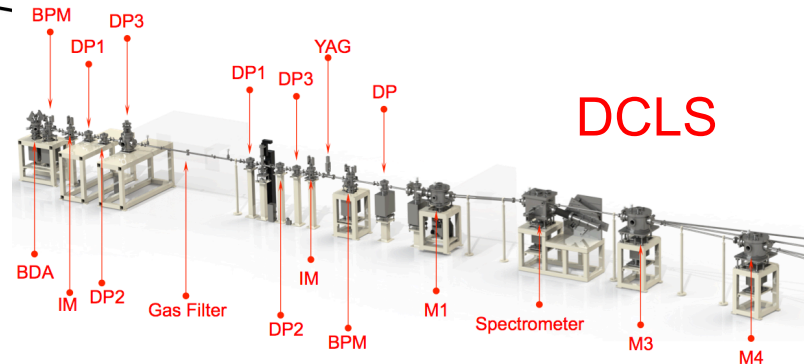
# FERMI



# FLASH



# DCLS



- EUV/SXR tunable sources → **Reflective elements** (mirrors and gratings), in **grazing incidence**, with **single-layered optical coating**, in **UHV** ( $10^{-9}$ - $10^{-10}$  mbar)
- Distance from source + unfocused until the endstations + divergence → **“big” mirrors** (tens of cm)
- **Quality of optics**: good but not necessarily as good as XFELs' ones (100's-nrad slope errors; 1-3 Å roughness)
- **One experiment per time** (possible exceptions by wavefront splitting or serial endstations)
- **Online and transparent diagnostics** → gas-based and/or grating-based
- Parameters to determine:  
**intensity, spectrum, position, mode, spot size, wavefront, polarization, pulse length, arrival time**
- Intensity/spectral content manipulation → gas and solid state **filtering**
- Focal spot manipulation sometimes necessary → **active optics** systems
- Transmission optimization → **mirror coating** selection



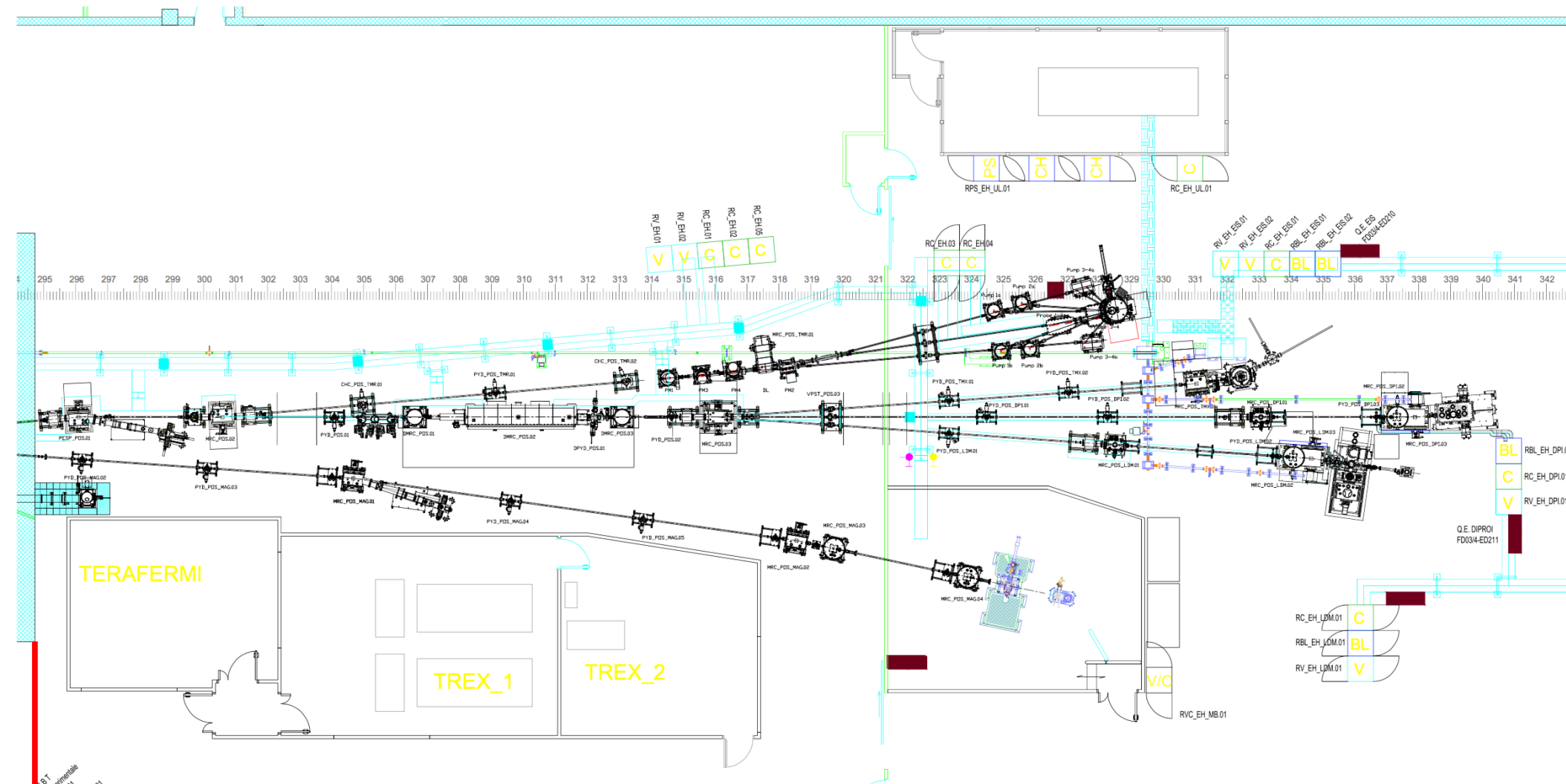


Elettra  
Sincrotrone  
Trieste

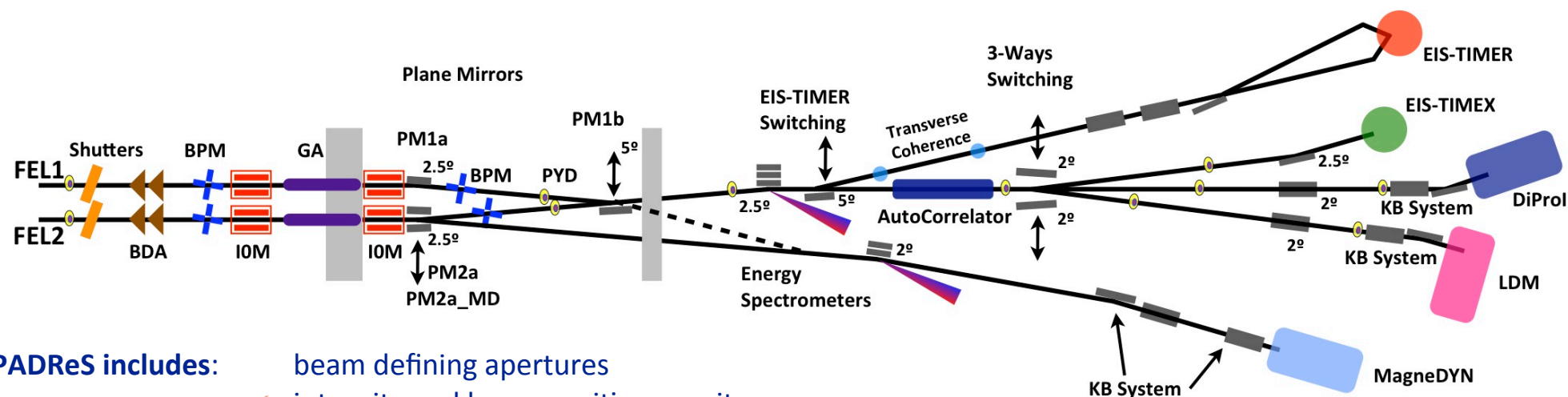


FERMI

# The experimental hall

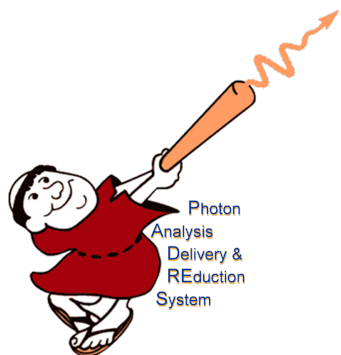






## PADReS includes:

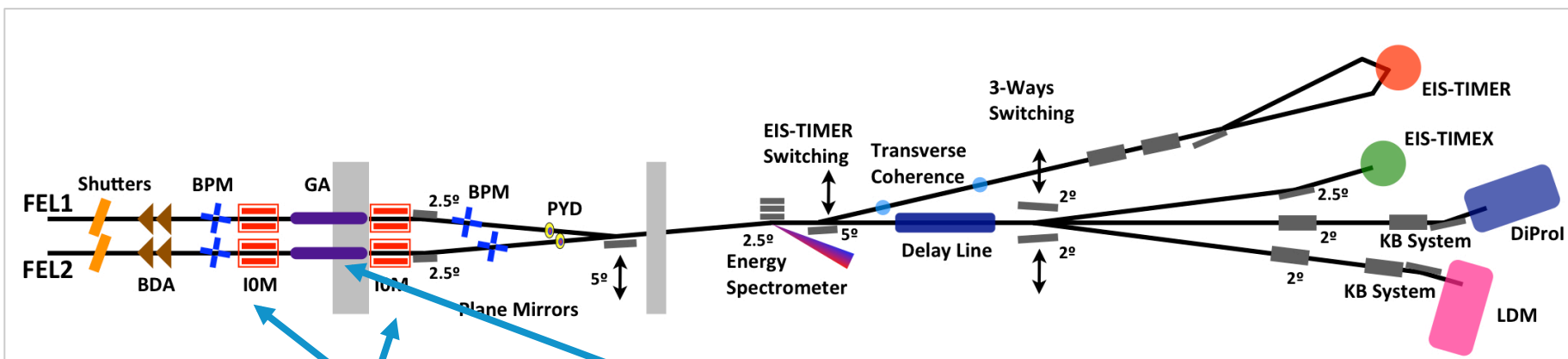
- beam defining apertures
- intensity and beam position monitors
- YAG screens and photodiodes
- intensity reducer
- energy spectrometer
- transverse coherence measurement
- split and delay line
- filters
- refocusing systems



## FERMI experience:

At the beginning (from CDR to first user Runs) the diagnostics had been “confined” to initial part of the transport. Run after Run it became clear that some **diagnostics** (e.g., intensity monitors) should be **replicated and installed all along the transport**



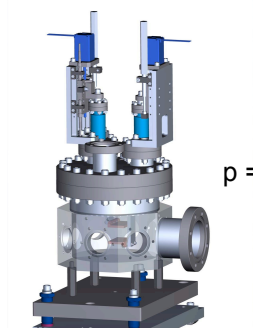


### Intensity monitors:

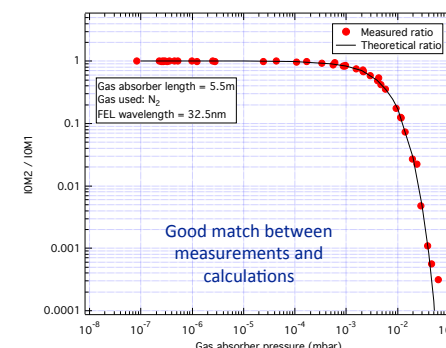
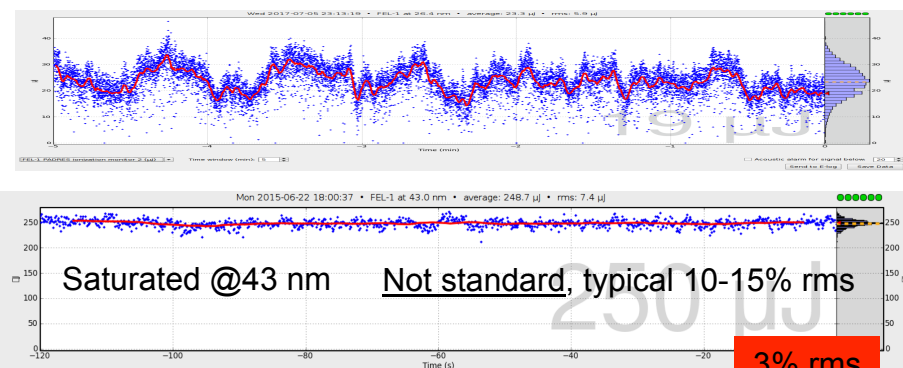
Measures the **number of photons of each pulse** (~3% precision, 1% reproducibility)  
Online and shot-to-shot  
Transparent

### Gas absorber:

Need to align the beam w/out destroying the sample + intensity-dependent studies  
**Max attenuation** at all  $\lambda$ :  $10^{-4}$   
Preservation of coherence, spectrum, statistics, etc.



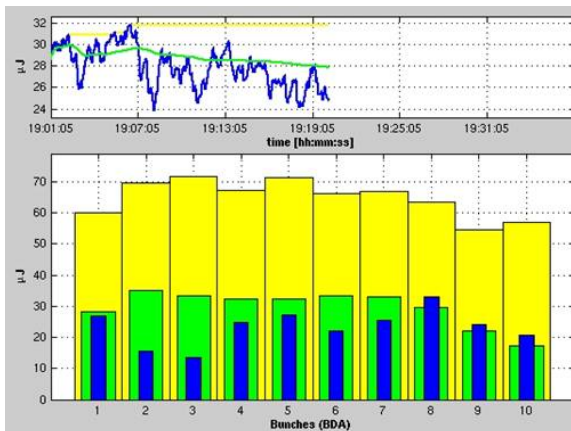
$p = 2 \cdot 10^{-5}$  mbar



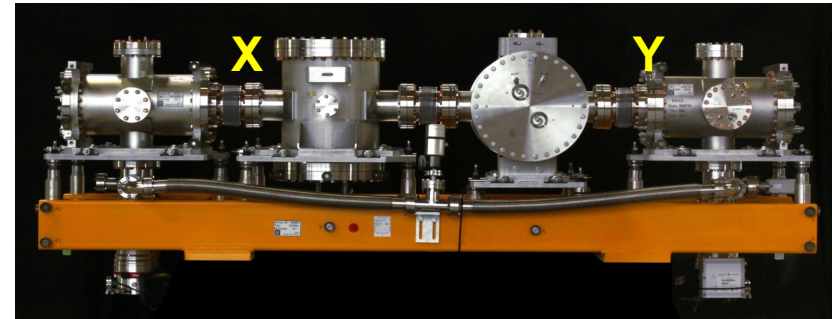
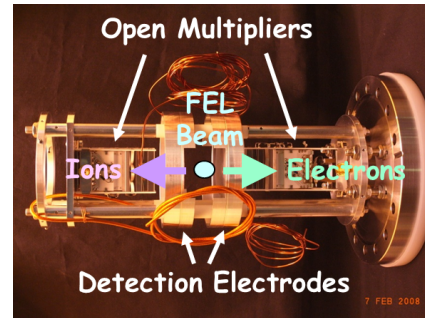
### FERMI experience:

**IOMs** should be **diversified** (gas-based, grating-based, mirror photo-current, operating on residual vacuum) and **distributed** along the transport (especially before the endstations)

### 1<sup>st</sup> generation GMD (FLASH1)

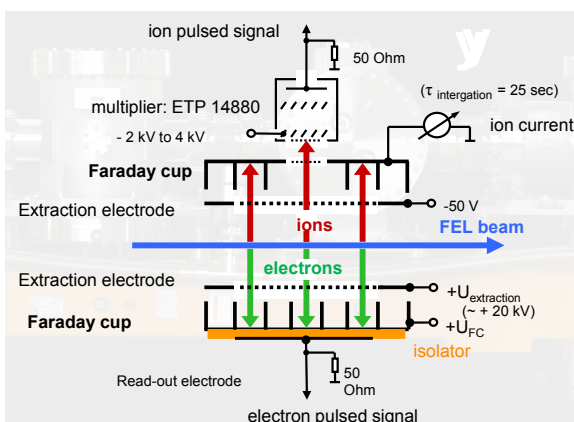
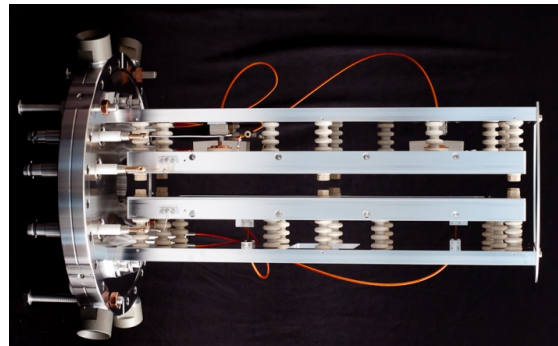


### Advanced GMD (round-robin) 3<sup>rd</sup> generation GMD (XFEL, FLASH2)



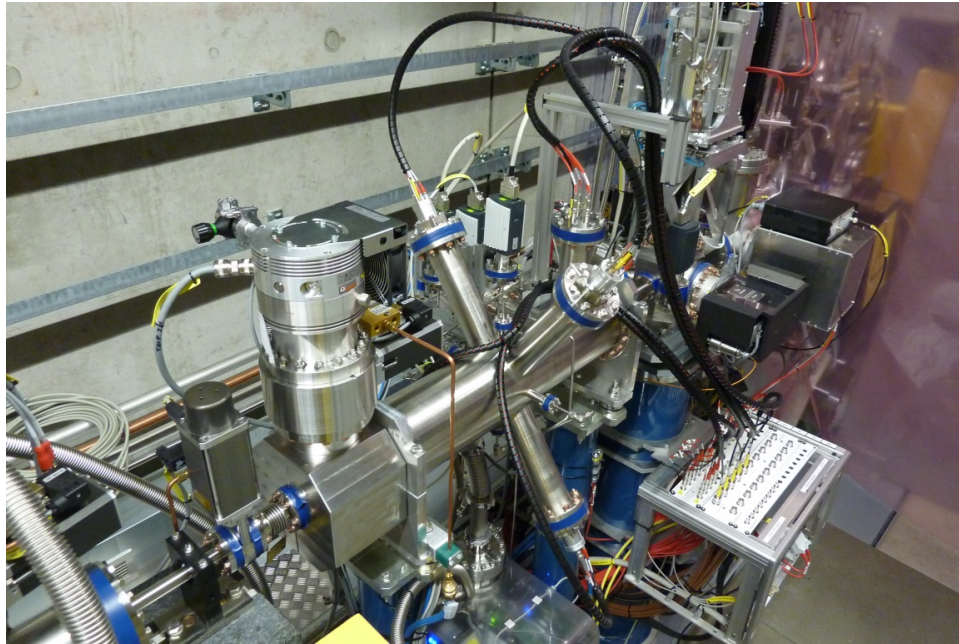
XGMD HAMP HAMP XGMD

- New XGM design copes with enhanced demands of the XFEL wavelength range:
  - higher sensitivity (larger XGMD absorption length)
  - higher dynamic range (tunable HAMP stage voltages)
- Test runs gases at the Willy-Wien-Labor, PTB Berlin
- Measurement of absolute ionization cross sections of rare gases at the PTB beamline at BESSY



Courtesy of K. Tiedtke and E. Plönjes (DESY)

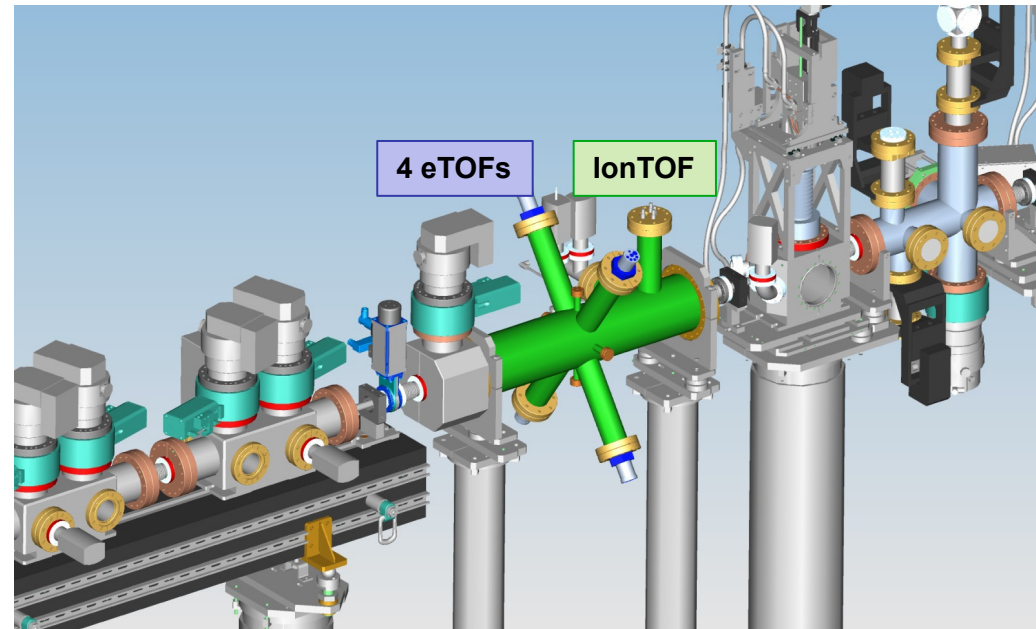
# WAVELENGTH (AND BANDWIDTH) FLASH2 OPIS



- Transmission: ~100%
- Signal recording by fast ADCs:  
Capable of operation with MHz  
repetition rate of the FLASH  
burst-mode
- Self-Calibration  
using Auger processes
- Accuracy better than 0.1nm

M.Braune et al., *J. Synchrotron Rad.* **23**, 10 (2016)

- 4 Electron time-of-flight spectrometers  
1 Ion time-of-flight spectrometer
- $\mu$ -metal chamber
- low target gas operation pressure:  
 $p_{\text{target}} \approx 10^{-7}$  hPa



Courtesy of M. Braune (DESY)



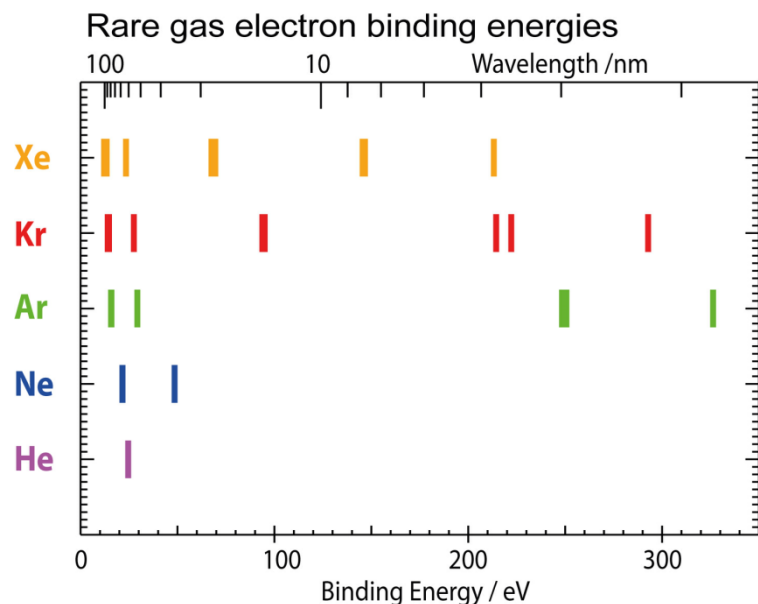
## WAVELENGTH (AND BANDWIDTH) FLASH2 OPIs

## > Electrons

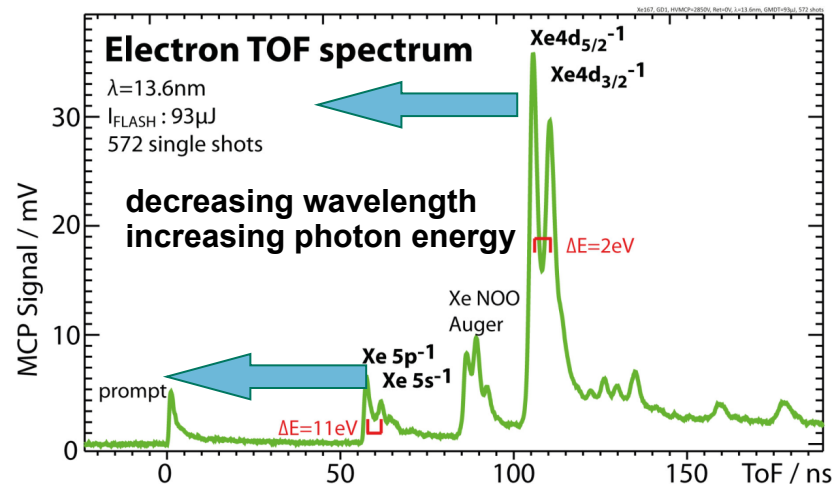
## Determination of the kinetic energy of photoelectrons directly from the flight time

$$E_{FEL} = E_{kin} + E_{bind}, \lambda_{FEL} = hc/E_{FEL}$$

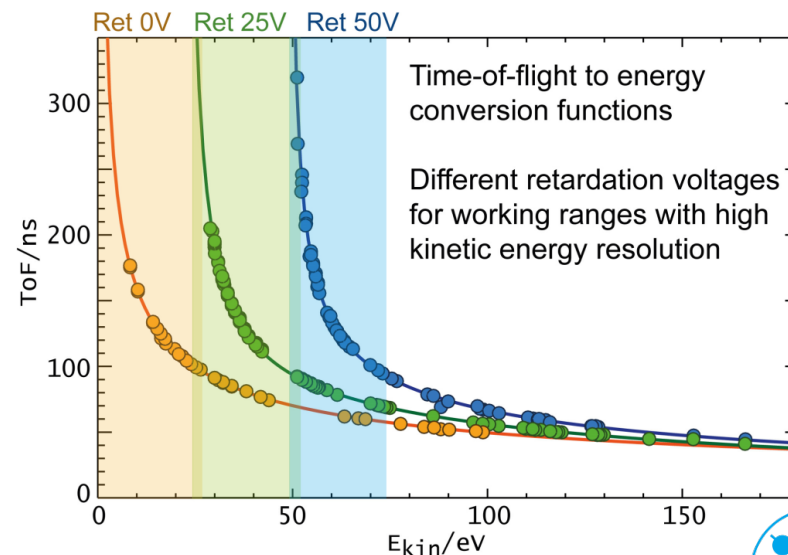
Various targets: rare gases  
Binding energy: literature



Advantages:  
operational in the full FLASH wavelength range  
measuring the complete wavelength range



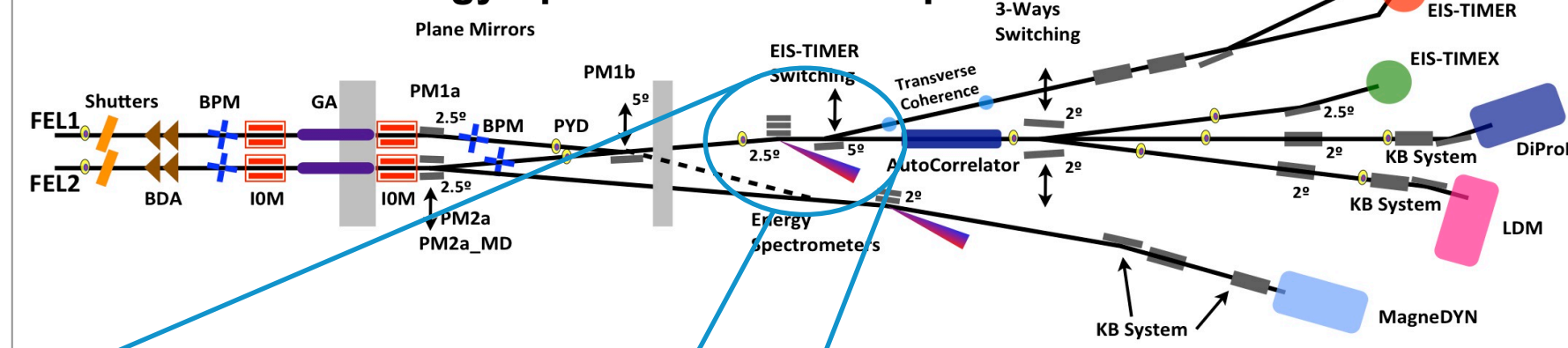
*X-ray data booklet, xdb.lbl.qov*



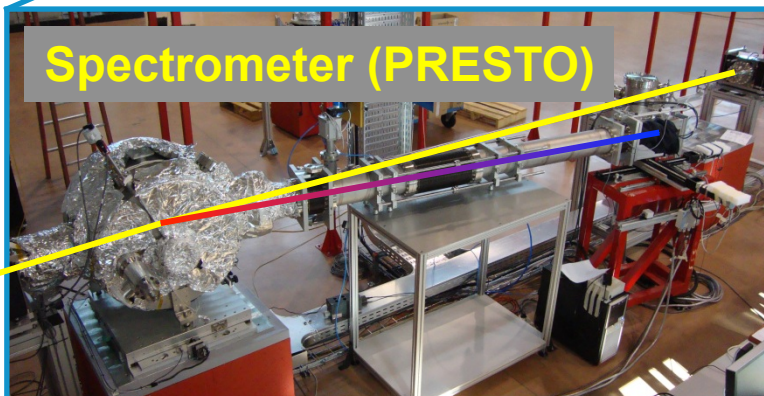
Possible error sources: external magnetic and electric fields  
**space charge**

Courtesy of M. Braune (DESY)

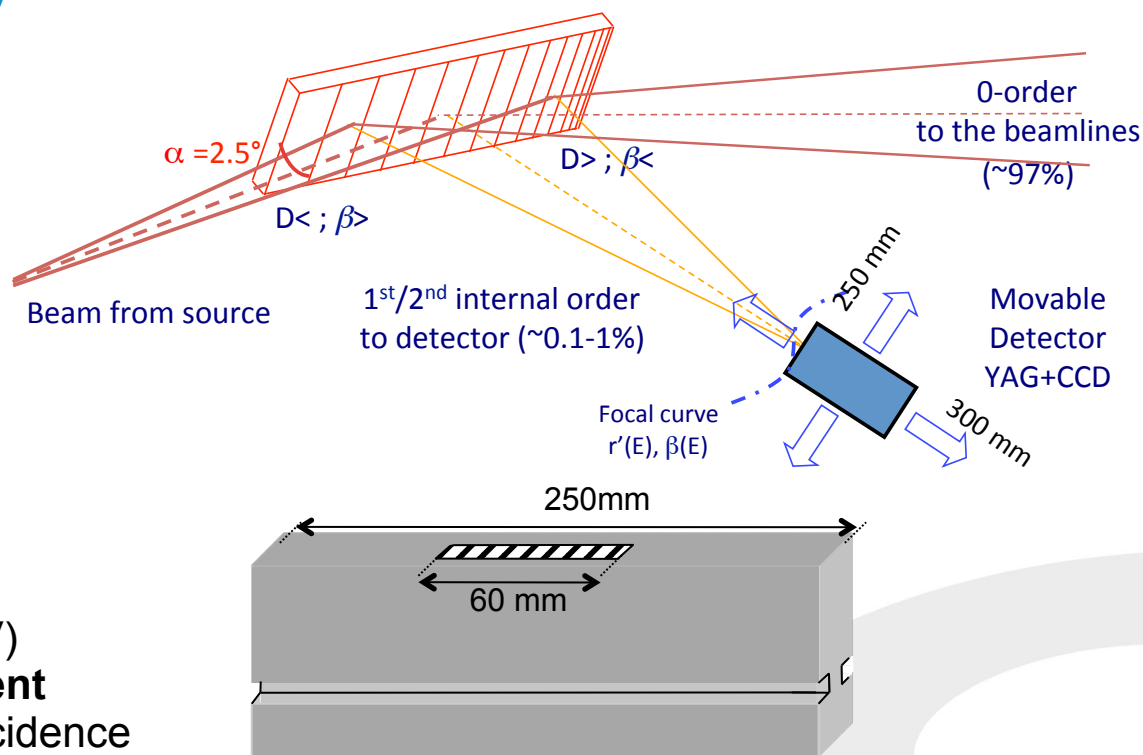
## Pulse-Resolved Energy Spectrometer: Transparent and Online



### Spectrometer (PRESTO)



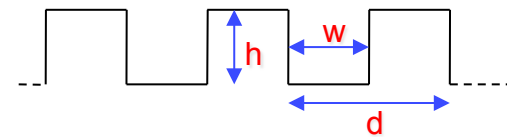
- **Online (non invasive)**
- Shot-to-Shot
- ~97% of FEL → beamlines
- 1% of FEL → YAG + triggered CCD
- Resolving Power ~15000 @32.5nm (2.5meV)
- Available information:  $\lambda$ , BW, spectral content
- **3 gratings** (Au, C and Ni coatings) – 2.5°-incidence



### Requests:

Fused silica substrate  
250x25mm<sup>2</sup> surface (240x17 active)  
Laminar profile – Central 60mm ruled  
Tang. Slope error rms <1μrad  
Radius of curvature >30km

h = groove depth  
w = groove width  
d = groove spacing



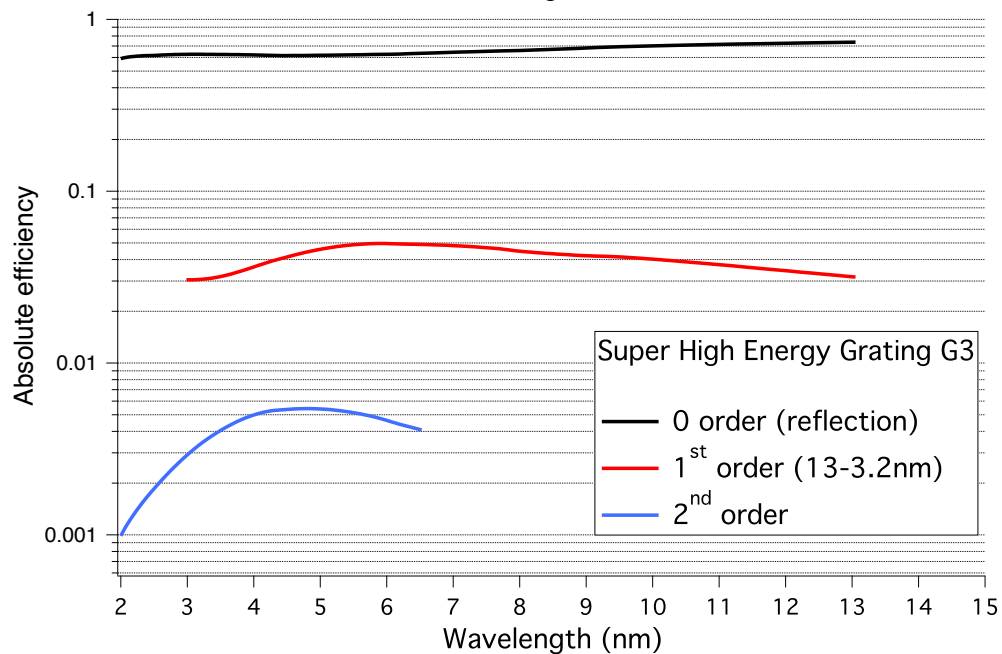
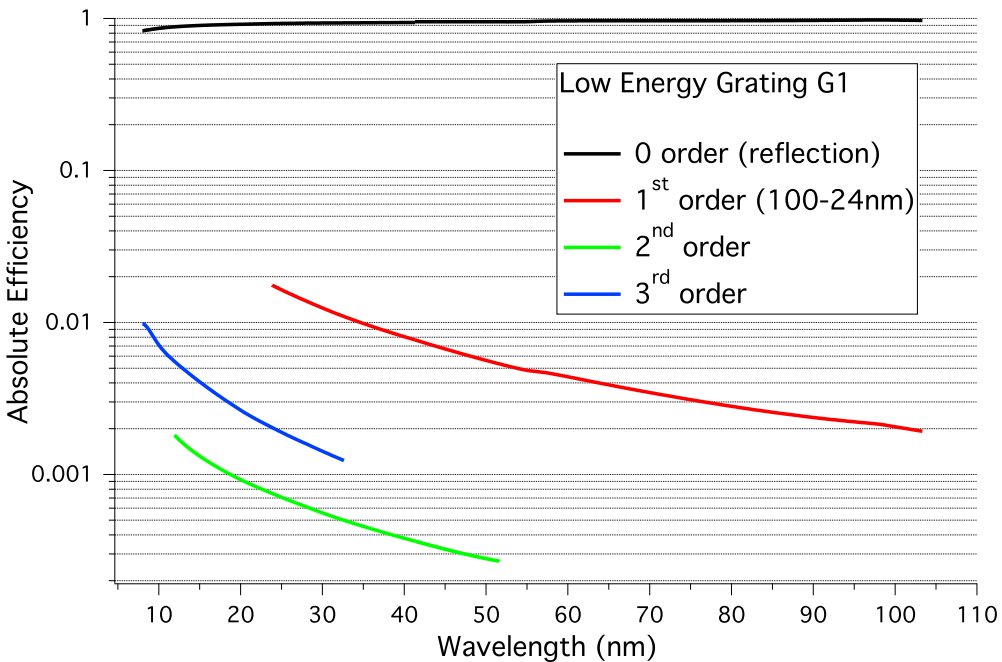
	LE	HE	SHE
Wavelength (nm)	100 – 24	27 – 6.7	13 – 3.2
Slope error rms (μrad)	0.28	0.28	0.32
Radius (km)	22	31	43
D <sub>0</sub> (l/mm)	500	1800	<b>3750</b>
D <sub>1</sub> (l/mm <sup>2</sup> )	0.35	1.26	2.68
D <sub>2</sub> (l/mm <sup>3</sup> )	1.7 · 10 <sup>-4</sup>	6.3 · 10 <sup>-4</sup>	1.4 · 10 <sup>-3</sup>
Groove height (nm)	12	4	8*
Groove ratio (w/d)	0.60	0.65	0.65**
Coating	Carbon	Gold	Nickel

**HORIBA** JOBIN YVON

\*Requested: 6nm – Offered: 8nm – Actual: 9nm

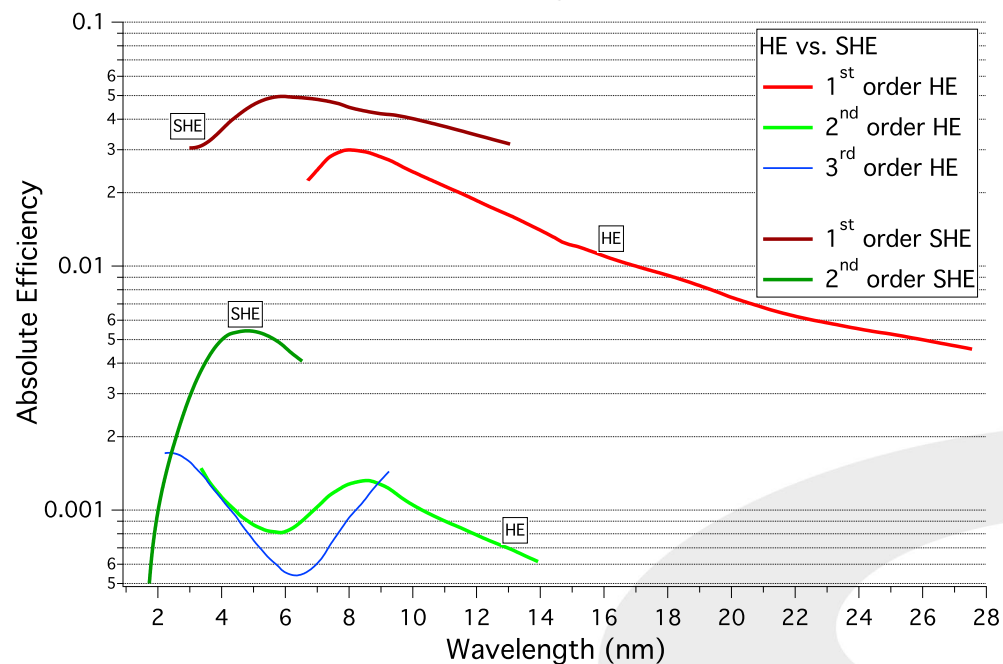
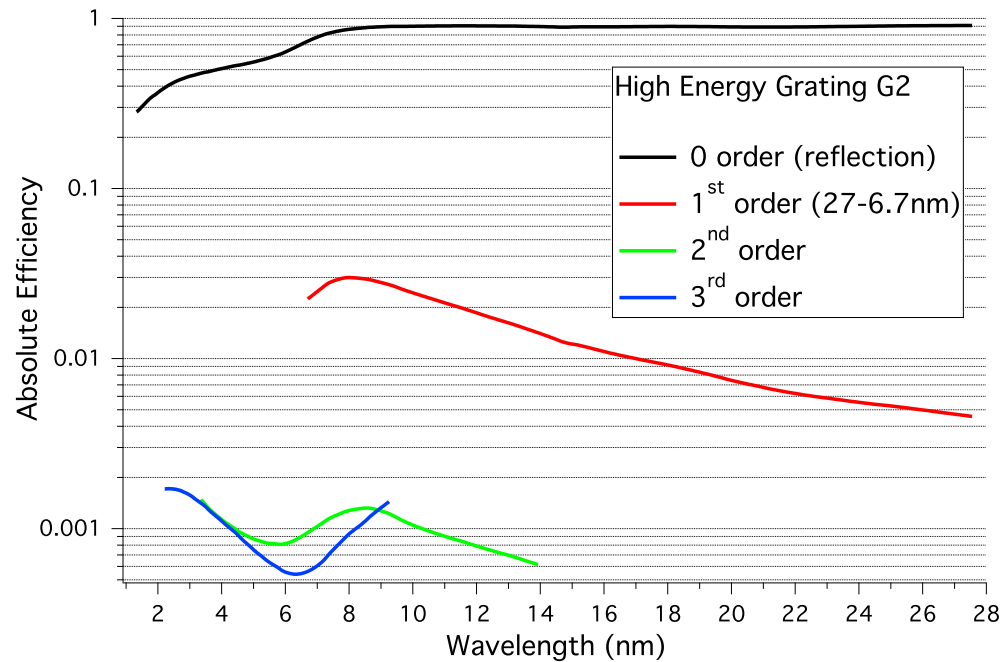
\*\*Requested: 0.8 – Offered: 0.65 – Actual: 0.65

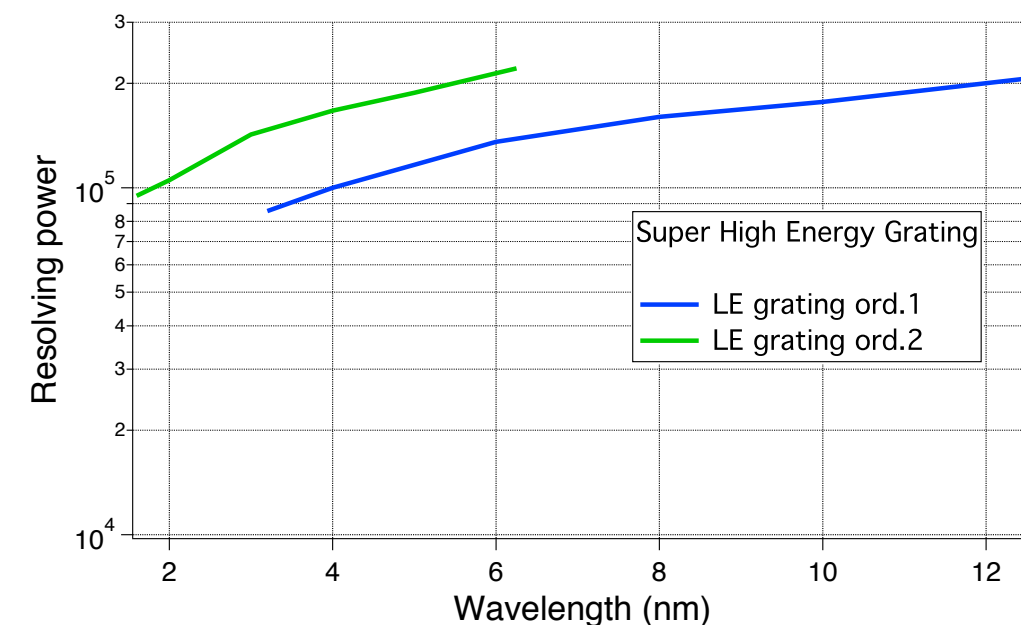
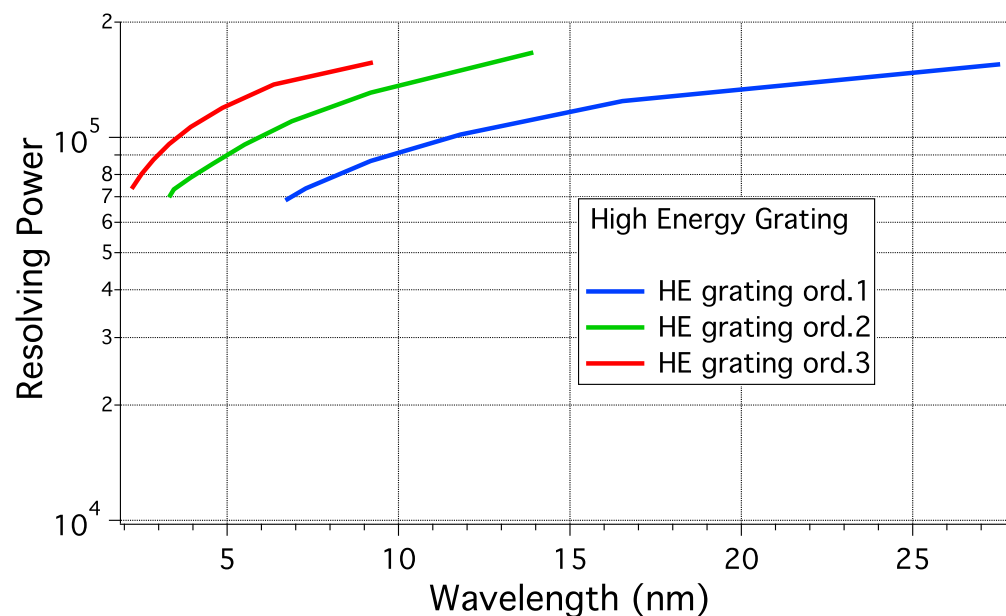
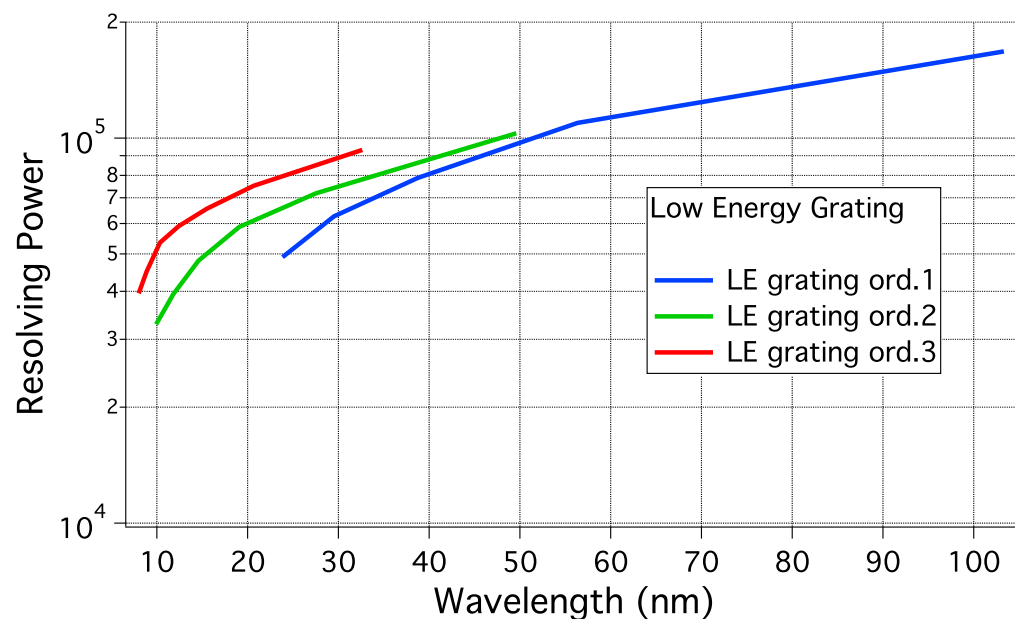




# PRESTO GRATINGS

## Efficiencies

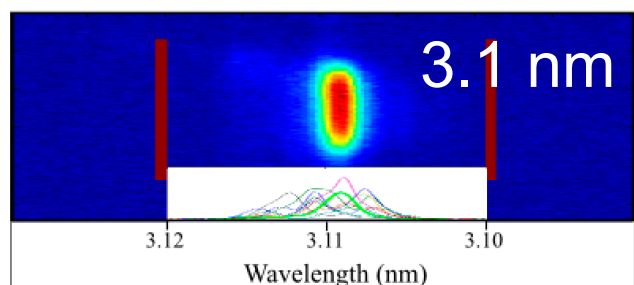
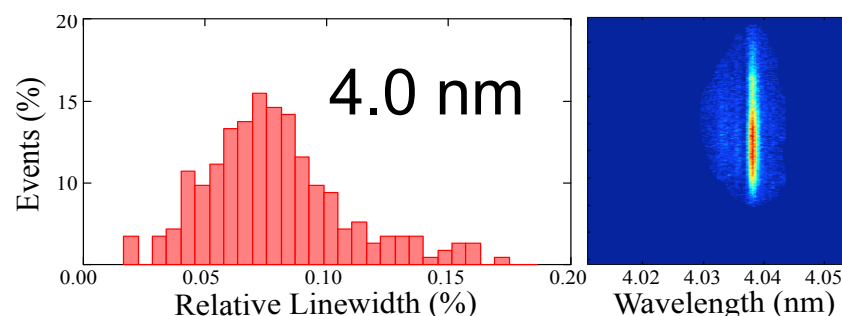
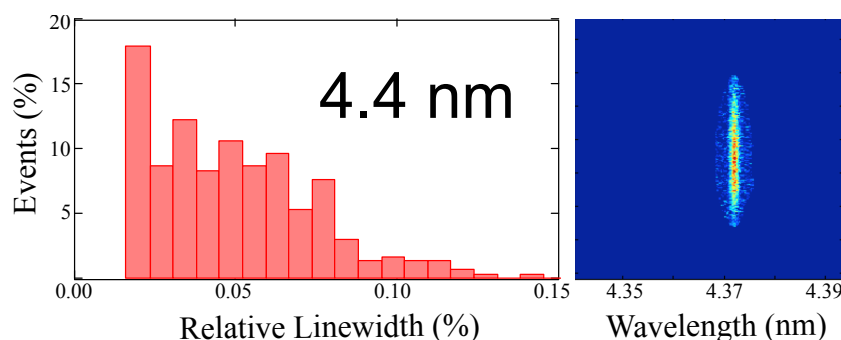
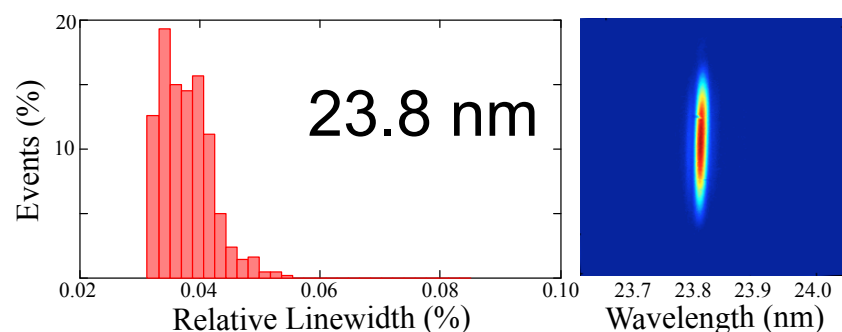
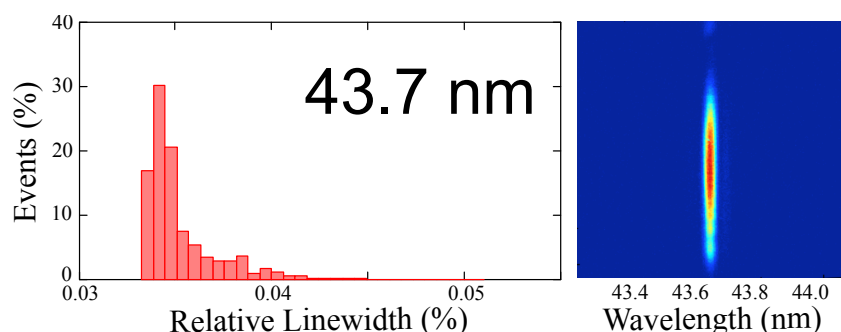




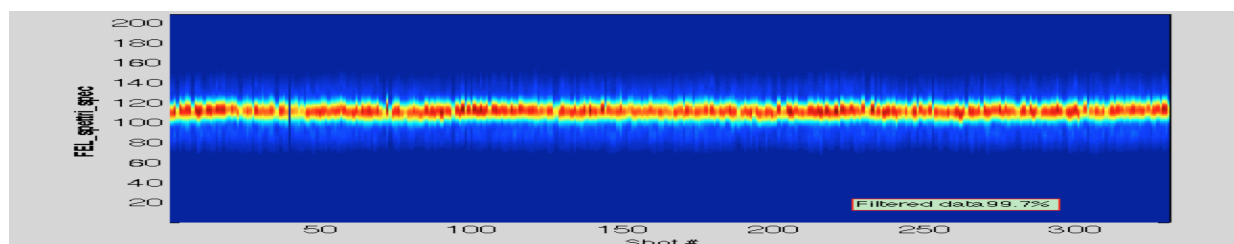
Resolving power to be scaled  
depending on the detection system

PRESTO currently uses a Ce:YAG in  
vacuum coupled to a visible light CCD  
camera → **Res.Power ~ 20.000**

Single shot **spectra** measured down to **4 nm** (even at 3.2nm); **narrow linewidth** with an **energy** per pulse at shorter wavelengths larger than **10  $\mu$ J**.



- **Gaussian with both wavelength and bandwidth stability.**



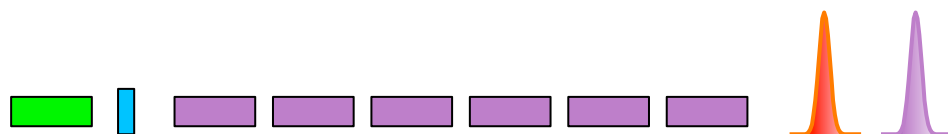
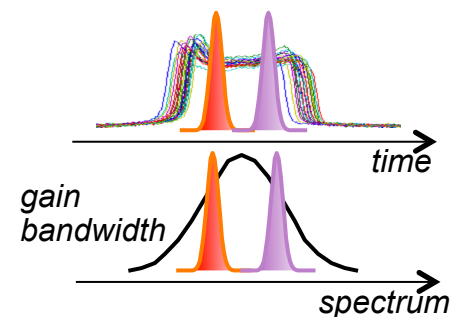


# TWO COLOR – TWO PULSES

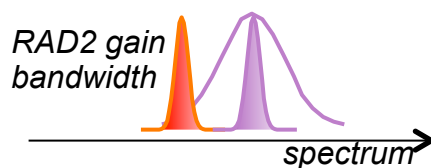
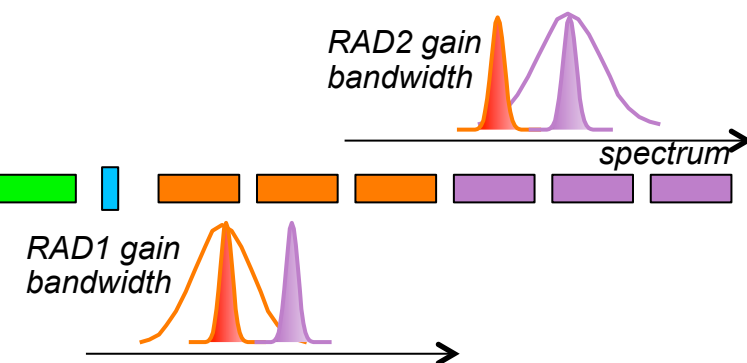
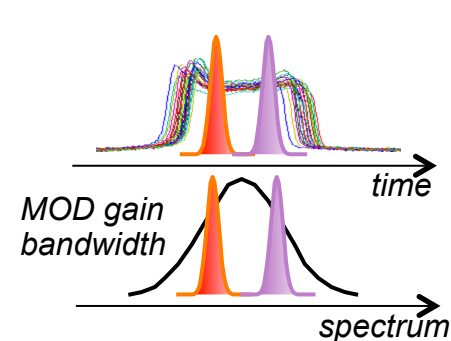
## Seeded FEL options

Multiple pulses can be generated by **double pulse seeding** in different ways, depending on the requirements on the output radiation. Temporal **separation between 25-300 and 700-800 fs**. Shorter separations are accessible via FEL pulse splitting\*. Larger separations require the split & delay line.

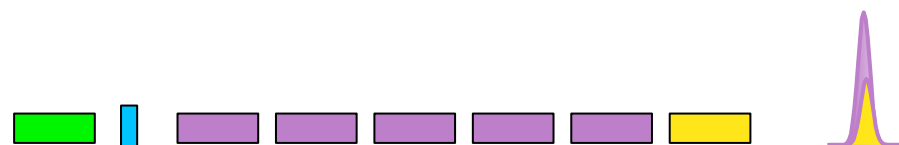
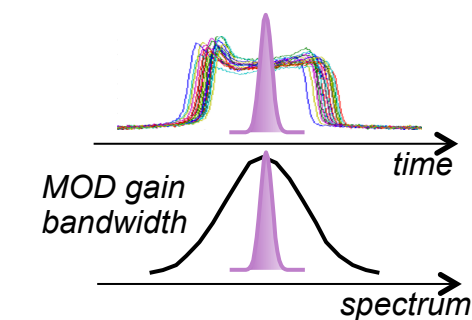
\* See e.g. Mahieu et al. Optics Express 21, 22728 (2013)



Spectral separation 0.4-0.7%  
(Capotondi)



Spectral separation 2-3%  
or much larger if the two  
radiators are tuned at  
different harmonics  
(Sacchi)



Two (almost) temporally  
superimposed pulses at  
harmonic wavelengths of  
the seed. The two pulses  
are correlated in phase and  
the phase can be  
controlled with the phase  
shifter (Prince)

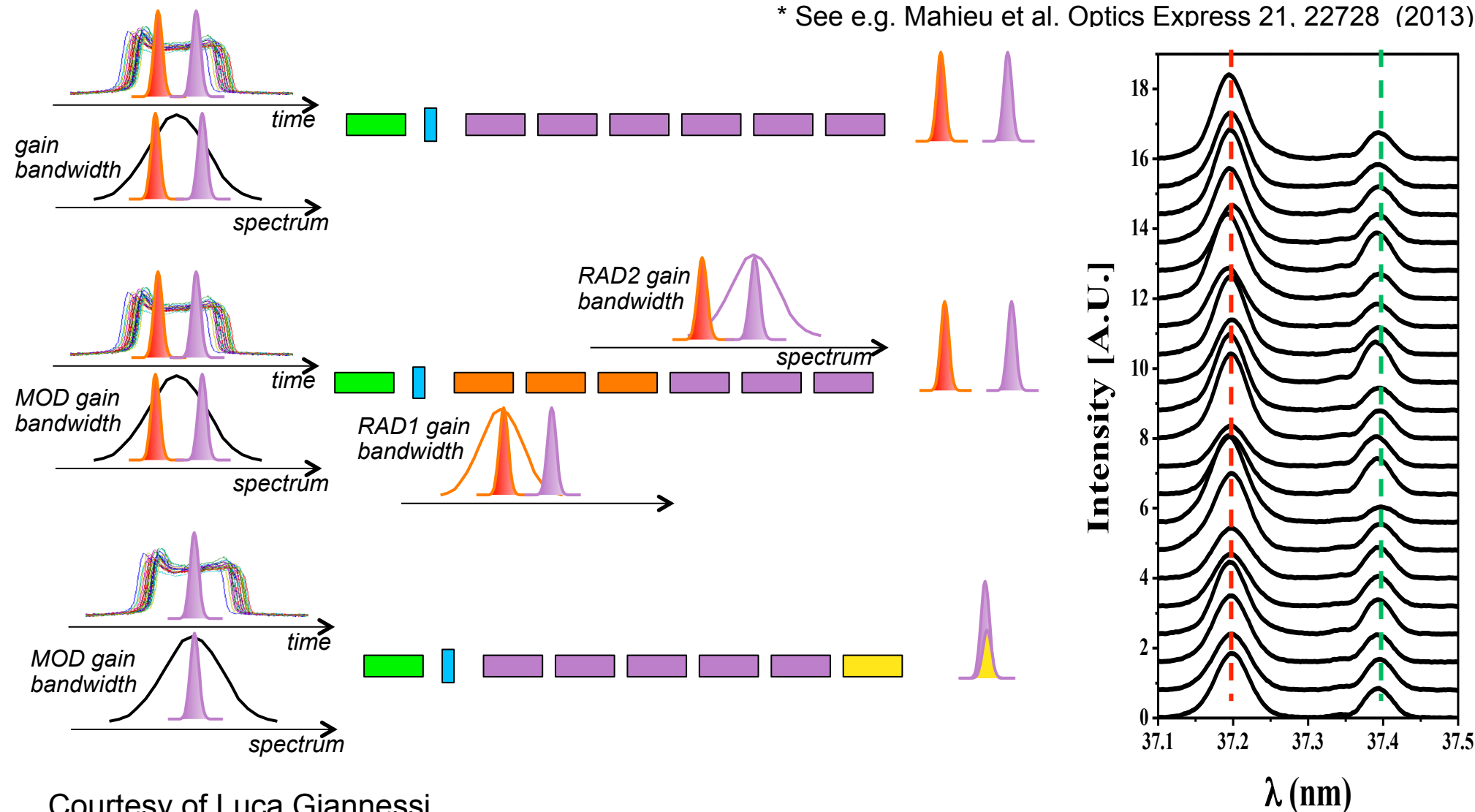
Courtesy of Luca Giannessi

# TWO COLOR – TWO PULSES

## Seeded FEL options

Multiple pulses can be generated by **double pulse seeding** in different ways, depending on the requirements on the output radiation. Temporal **separation between 25-300 and 700-800 fs**. Shorter separations are accessible via FEL pulse splitting\*. Larger separations require the split & delay line.

\* See e.g. Mahieu et al. Optics Express 21, 22728 (2013)



Courtesy of Luca Giannessi

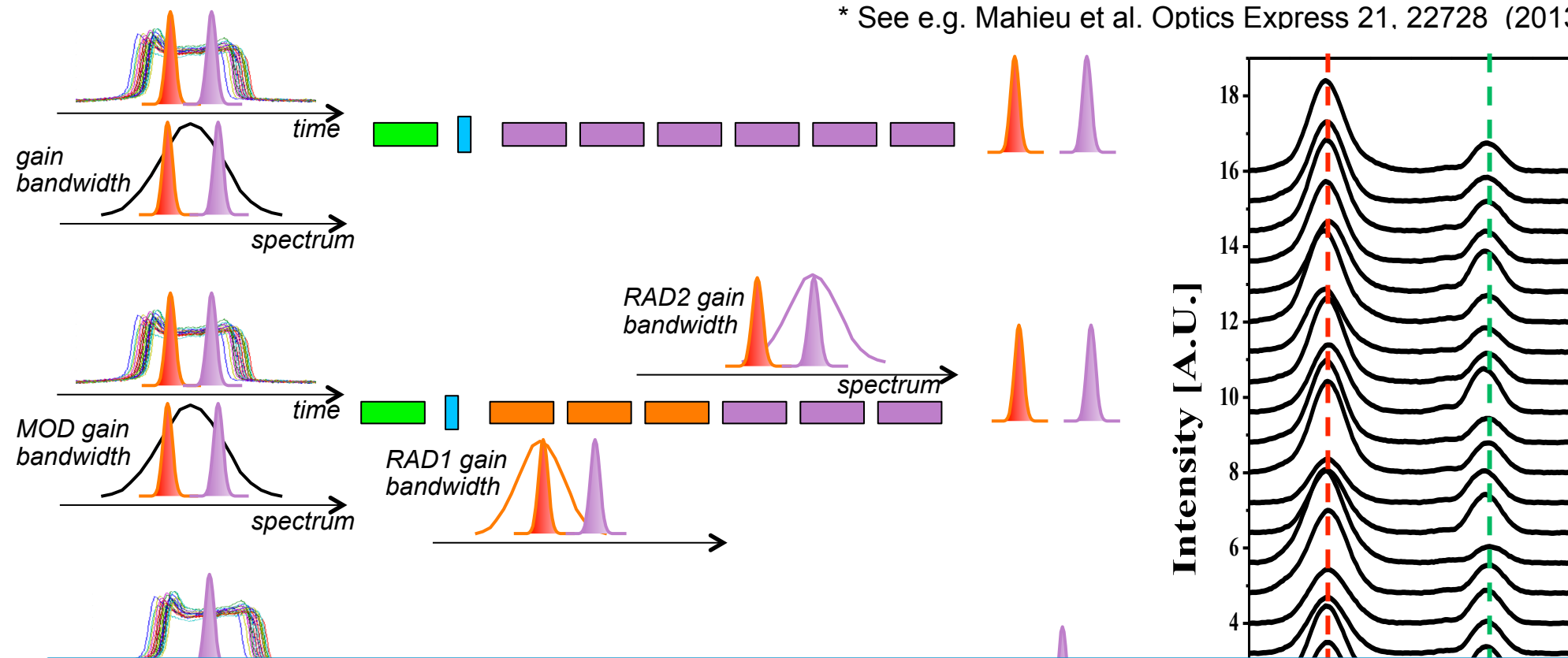


## TWO COLOR – TWO PULSES

### Seeded FEL options

Multiple pulses can be generated by **double pulse seeding** in different ways, depending on the requirements on the output radiation. Temporal **separation between 25-300 and 700-800 fs**. Shorter separations are accessible via FEL pulse splitting\*. Larger separations require the split & delay line.

\* See e.g. Mahieu et al. Optics Express 21, 22728 (2013)

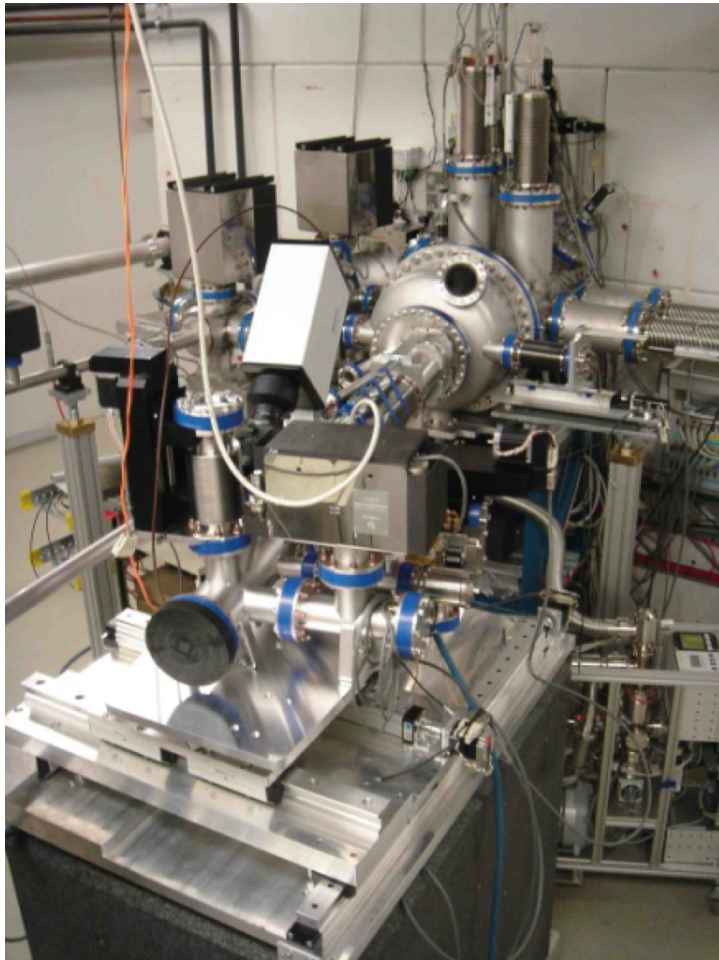


### FERMI experience:

The energy spectrometer should operate in single-shot mode (→ **efficient grating and detectors**) and should be able to operate in **two/multi color acquisition mode** to measure fundamental/higher harmonics, 2-color double pulses, and FEL double-stage photons

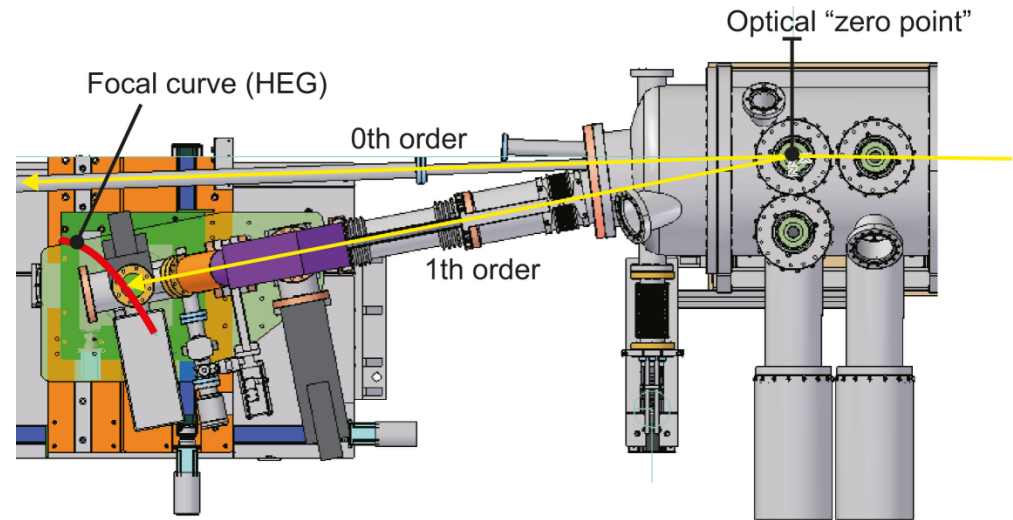
# SPECTRAL CONTENT

## FLASH VLS Grating Spectrometer



Permanent installation in the beam distribution area

G. Brenner et al., NIM A 635, S99-S103 (2011)



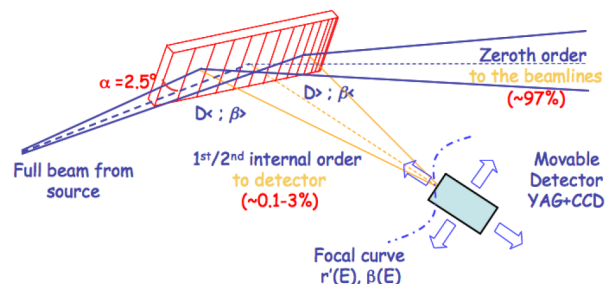
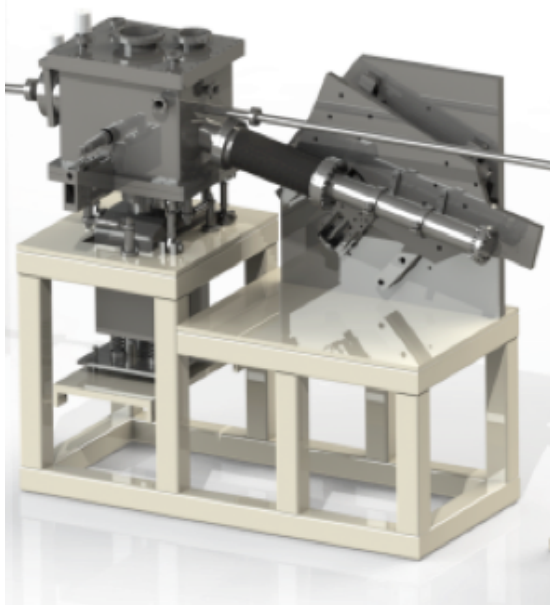
Grazing incidence design ( $2^\circ$  incidence angle)  
High and low energy VLS gratings (900 / 300 l/mm)  
Spectral range: 5.4 - 60 nm  
Resolution  $\approx 1500@25\text{nm}$  (design value  $>5000$ )

Additional plane mirror (Ni and C coatings)  
Mirror-mode:  
Full intensity to the experimental hall

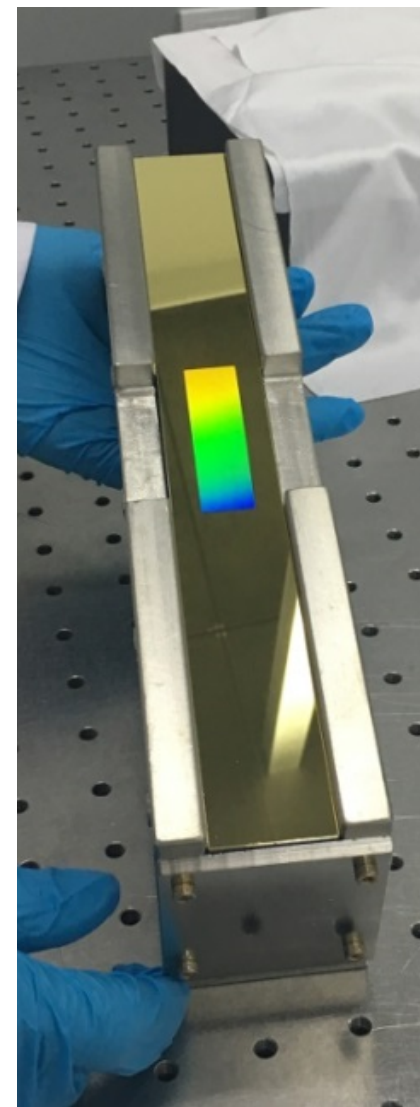
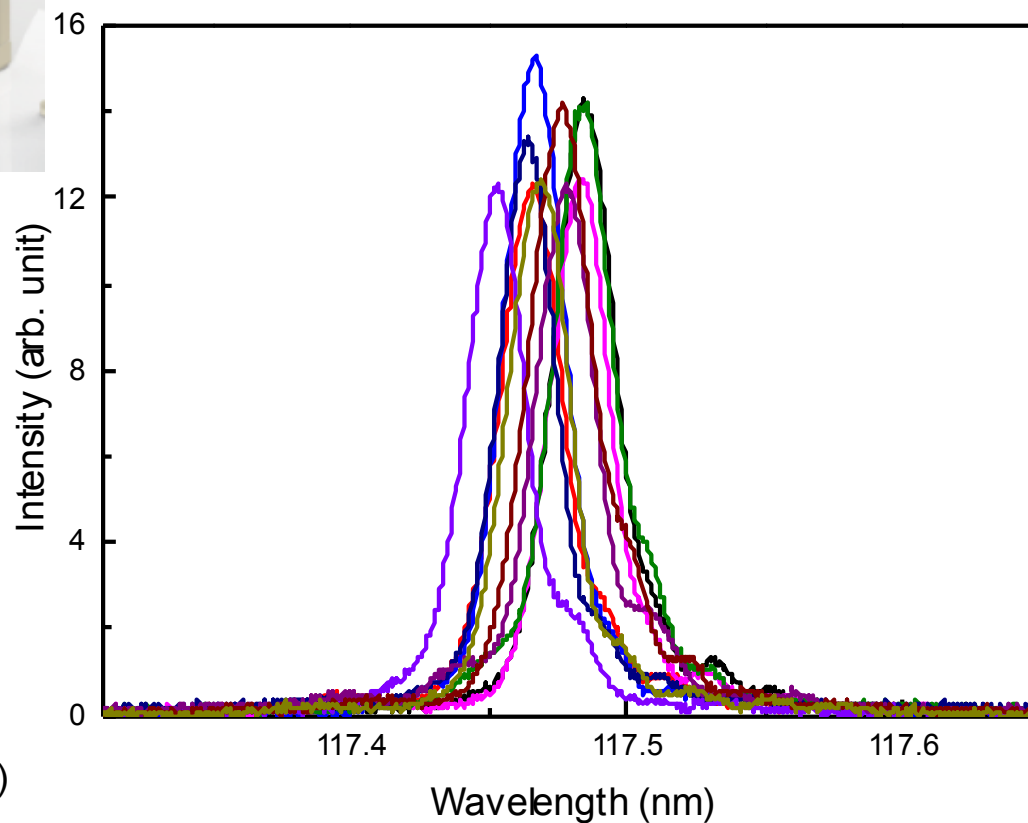
Spectrometer-mode:  
0<sup>th</sup> order: high transmission to exp. hall  
1<sup>st</sup> order: 1–10% of intensity for spectral analysis



Courtesy of G. Brenner (DESY)



- The resolution of spectrometer is designed as high as 14000.

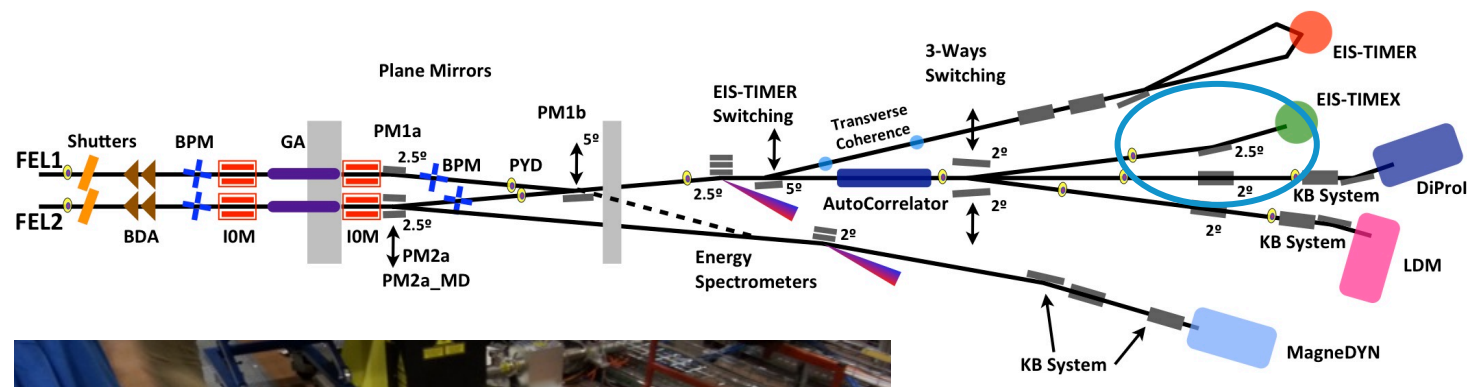


Courtesy of W. Zhang (DCLS)

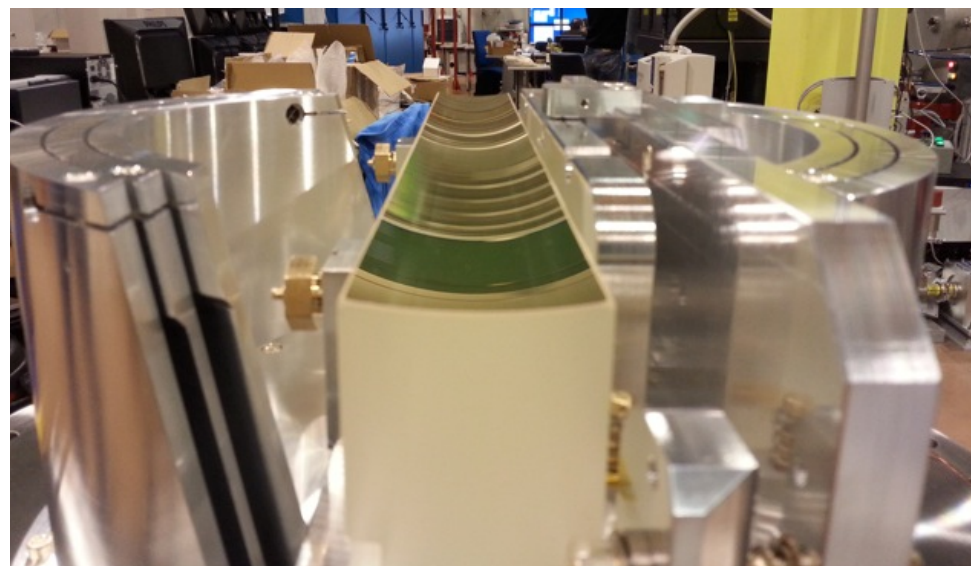
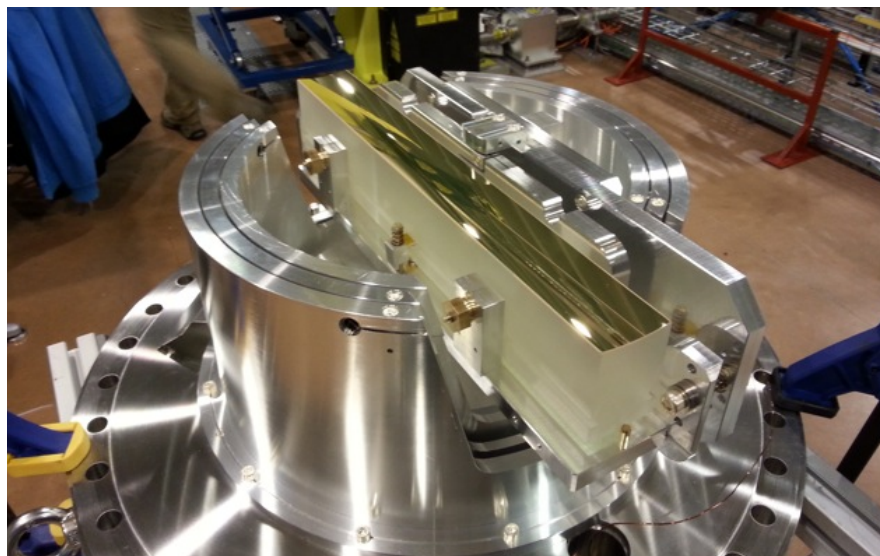
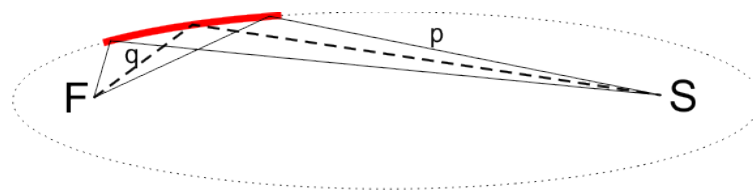


# PHOTON BEAM FOCUSING

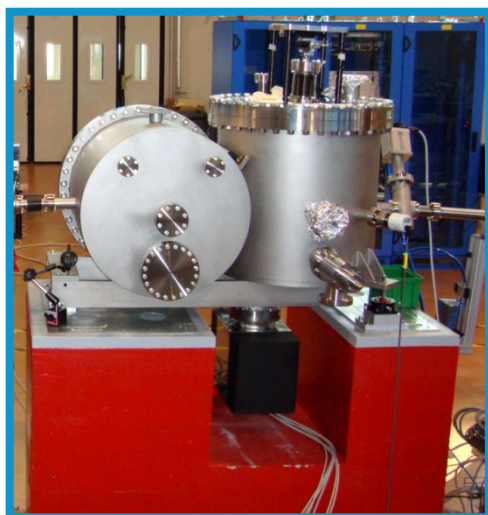
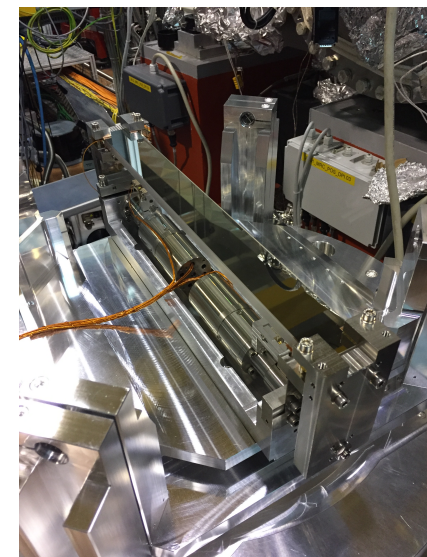
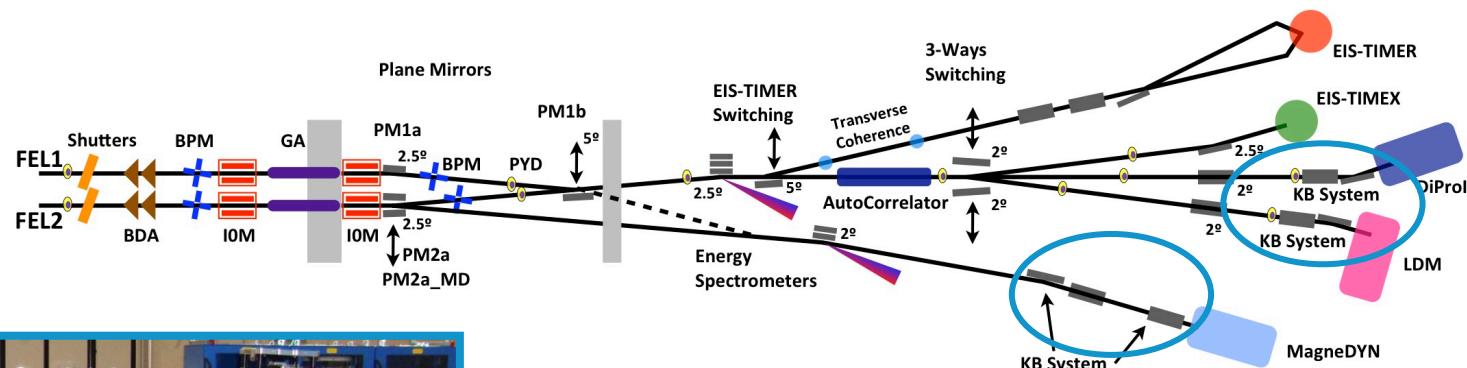
## Bulk Ellipsoidal Mirror



Entrance arm: 84.85 m  
Focal length: 1.4 m  
Incidence angle:  $2.5^\circ$

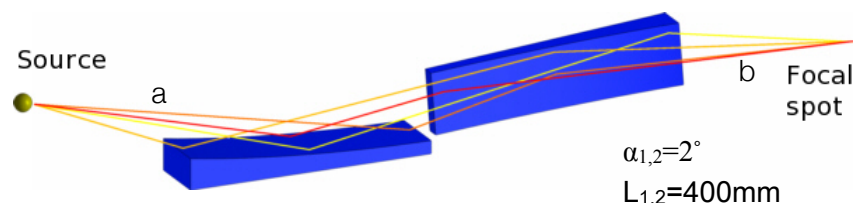


- **Single** ellipsoidal mirror (Hor. Deflecting)
- Optimized for FEL-2 (but focuses FEL-1 as well)
- Out-of-focus needed for FEL-external laser overlapping



### Kirkpatrick-Baez Active Optical Systems (KAOS):

- Active plane mirrors in **Kirkpatrick-Baez** configuration
- Focus **different sources** (FEL-1 and FEL-2) in **selectable positions**
- Decouple H from V focusing
- Adjustable to optimize focusing
- Adapt spot for FEL-external laser **overlapping**
- Optimize focal spot in **external user endstations**



$$a_{1,2} = 98754 - 99354 \text{ mm} \quad b_{1,2} = 1750 - 1200 \text{ mm}$$

**Entrance arm:** ~100 m  
**Focal length:** 1.2-1.75 m  
**Incidence angle:** 2°

- Best focusing  $\rightarrow$   **$\lambda$ -dependent** ( $\sim 2 \times 3 - 8 \times 8 \text{ } \mu\text{m}^2$ )
- **Defocusing** possible: from best focus to  $\sim 1 \times 1 \text{ mm}^2$

$\rightarrow$  Need for suitable diagnostics

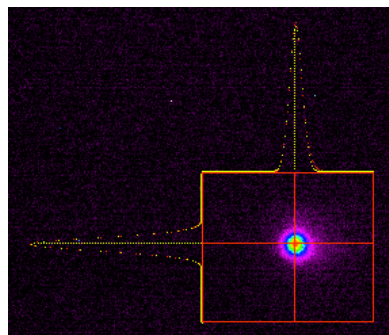


# SPOT SIZES DETERMINATION

## Different techniques

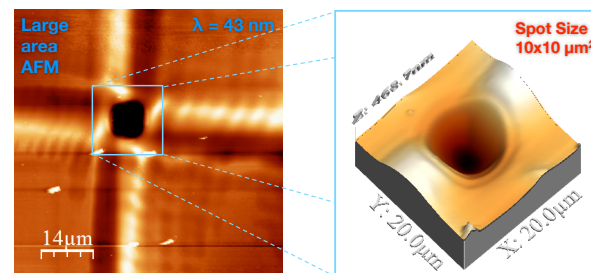
### Scintillator-based (e.g. Ce:YAG)

- Invasive
- May suffer from saturation effects
- Scintillator gets damaged in focus
- No single-shot information (generally)
- Quick and cheap



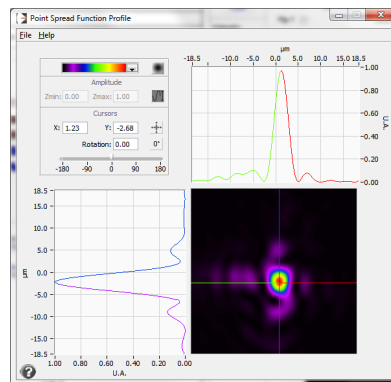
### PMMA and Si indentation

- Invasive
- Single shot information
- Deadly time-consuming (not fit for beamtimes)



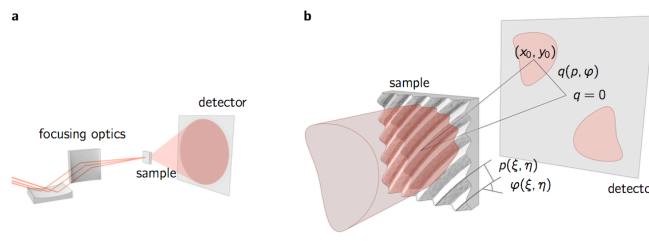
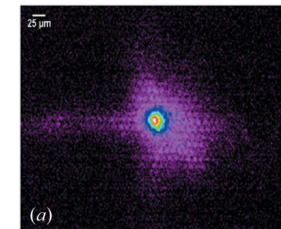
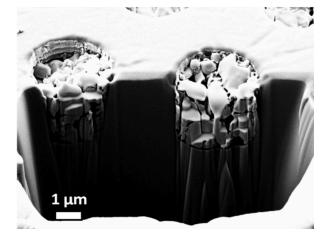
### Wavefront sensor

- Almost non invasive (intensity issues)
- Single shot information
- Online
- Quantitative information about focusing



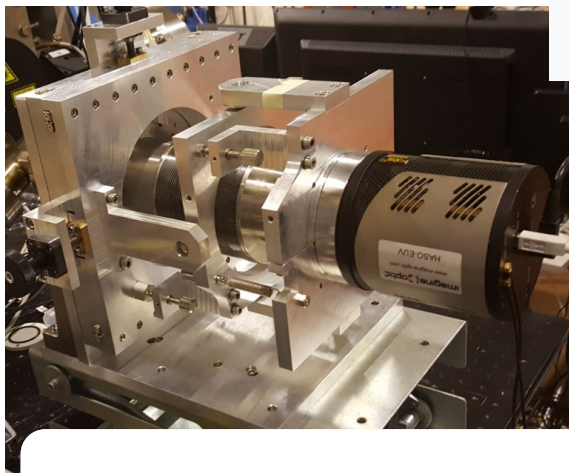
### Other techniques

- Pixelated P array  
(ref. A. Matruglio et al., J. Synchrotron Rad. (2016). 23, 29-34)
- VLS grating based spot reconstruction  
(ref. M.Schneider, et al., arXiv:1705.03814)
- ...

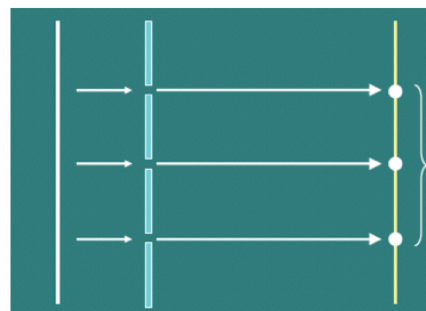


# SPOT SIZES DETERMINATION

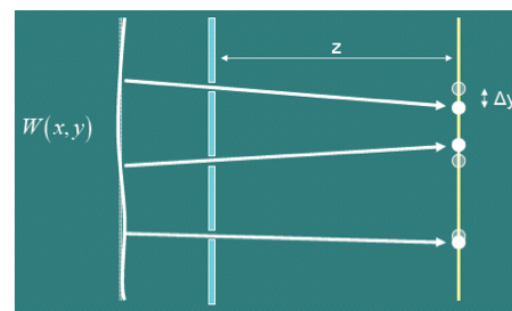
## Wavefront sensor



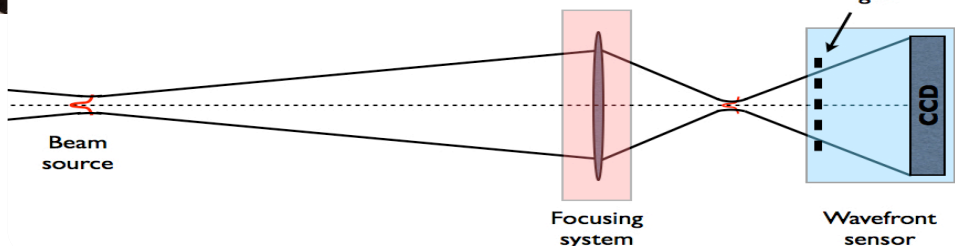
**Imagine Optic**



Wavefront Screen Reference spots on Detector

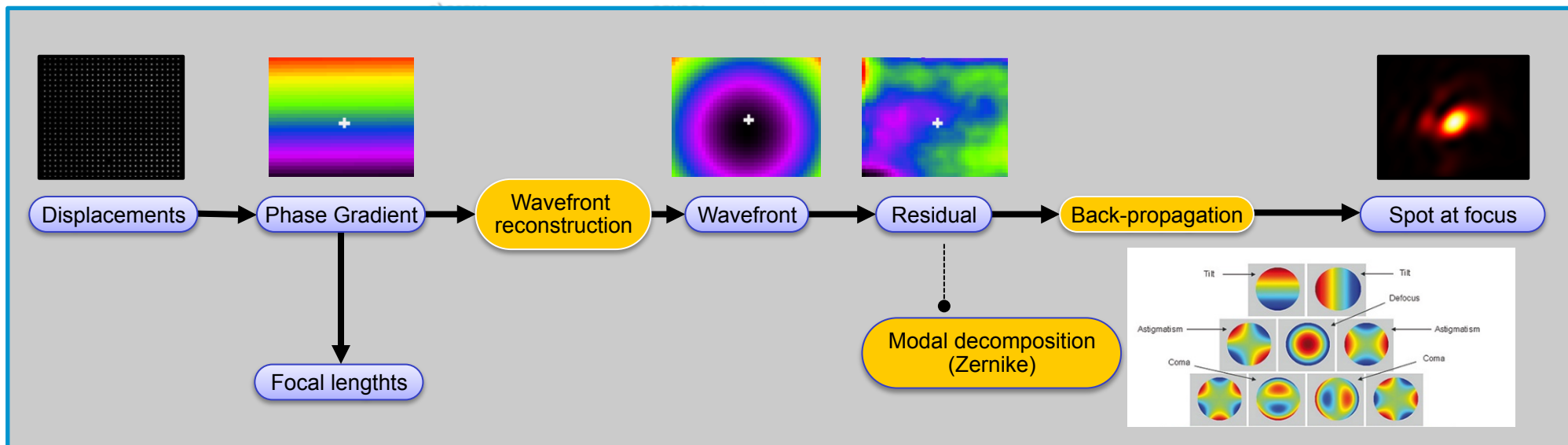


Slopes =  $\Delta y/z$



### SPECS

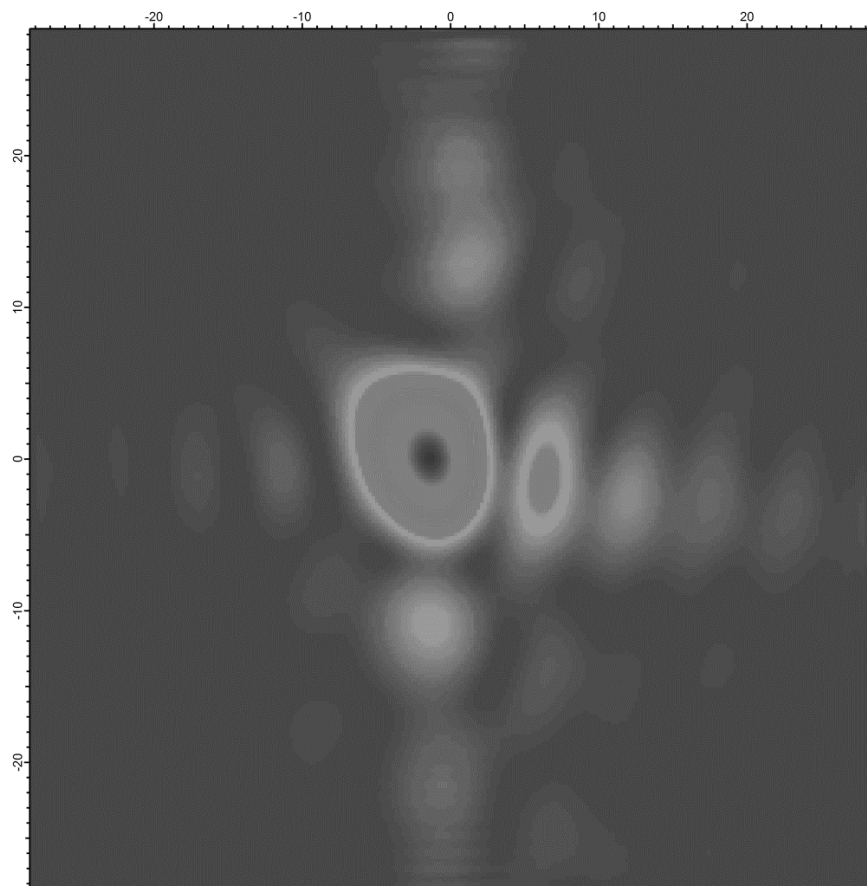
- 72 x 72 grid (13 x 13) mm<sup>2</sup>
- Pitch=180μm, Pinhole diameter: 60μm
- Wavelength range: 4-40nm
- Accuracy ~ $\lambda/10$
- Squared pinholes !





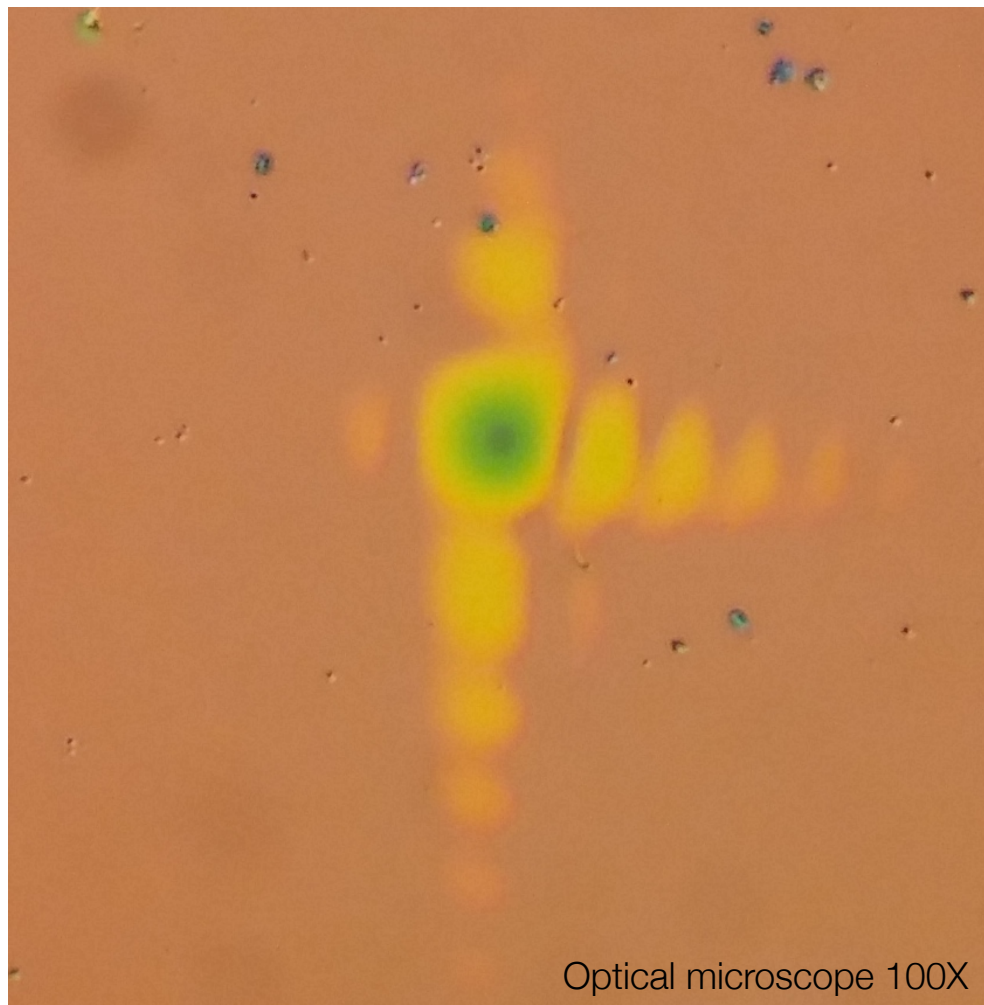
# SPOT DETERMINATION WFS vs. PMMA

Reconstruction from Hartmann WFS data



WFS reconstruction at 32nm: FWHM =  $5.7 \times 6.5 \mu\text{m}^2$

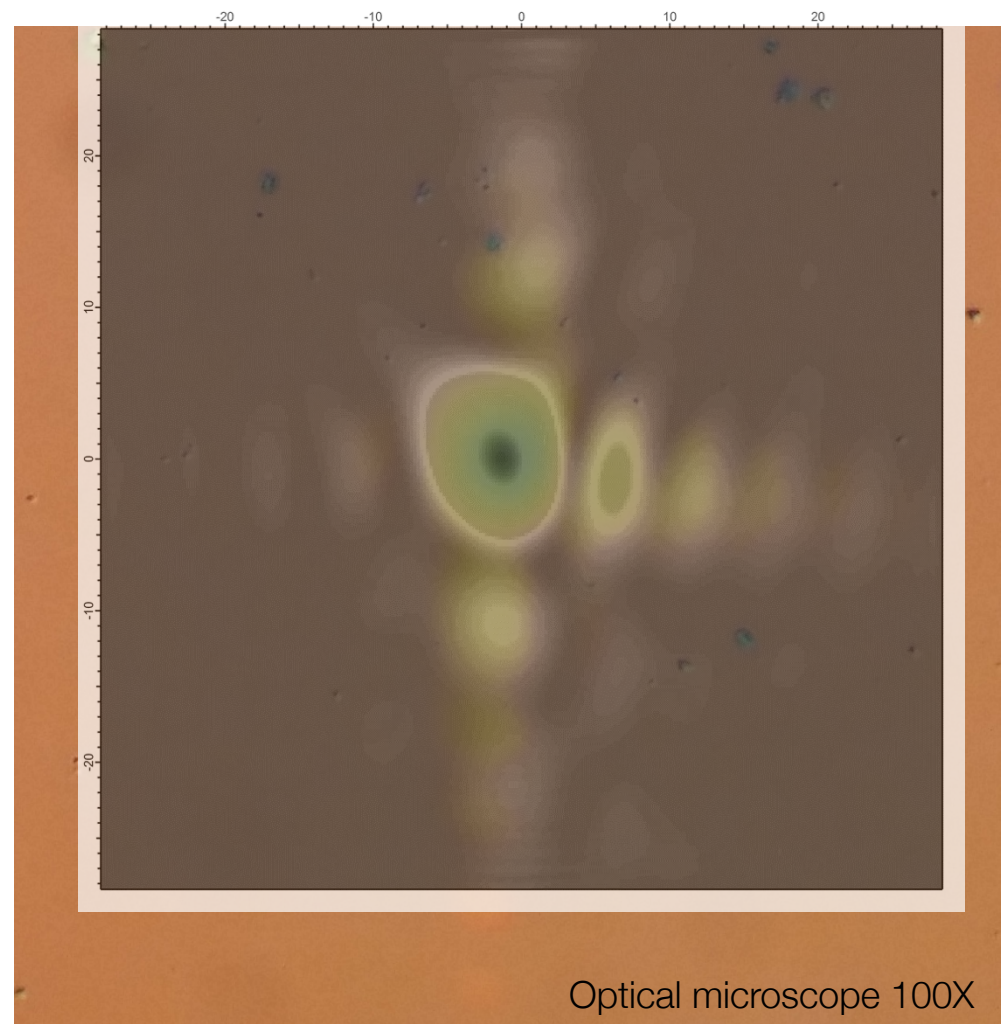
PMMA ablation imprint



Optical microscope 100X

# SPOT DETERMINATION WFS vs. PMMA

PMMA ablation imprint



**Good agreement** between in-house  
reconstruction and PMMA

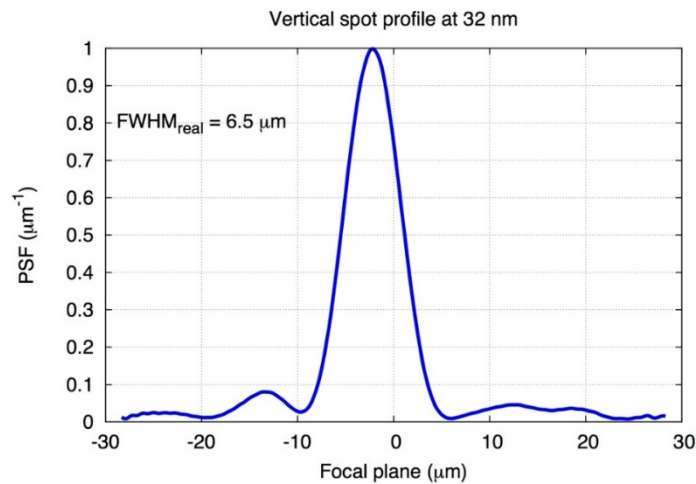
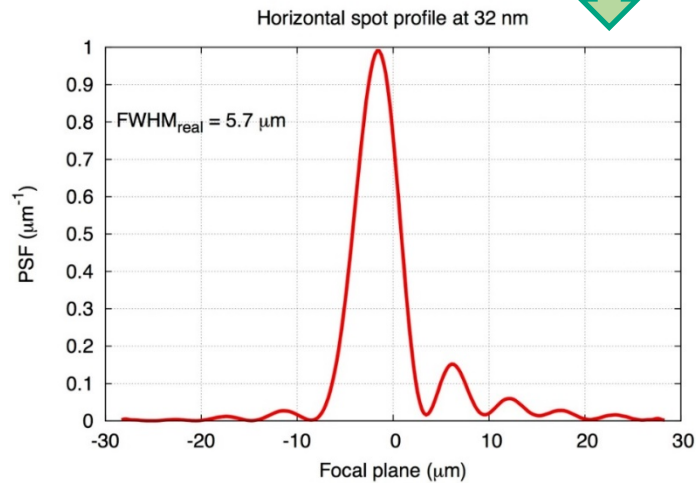


### Focal spot simulations from metrology

Profilometry at best  
curvature (LTP)

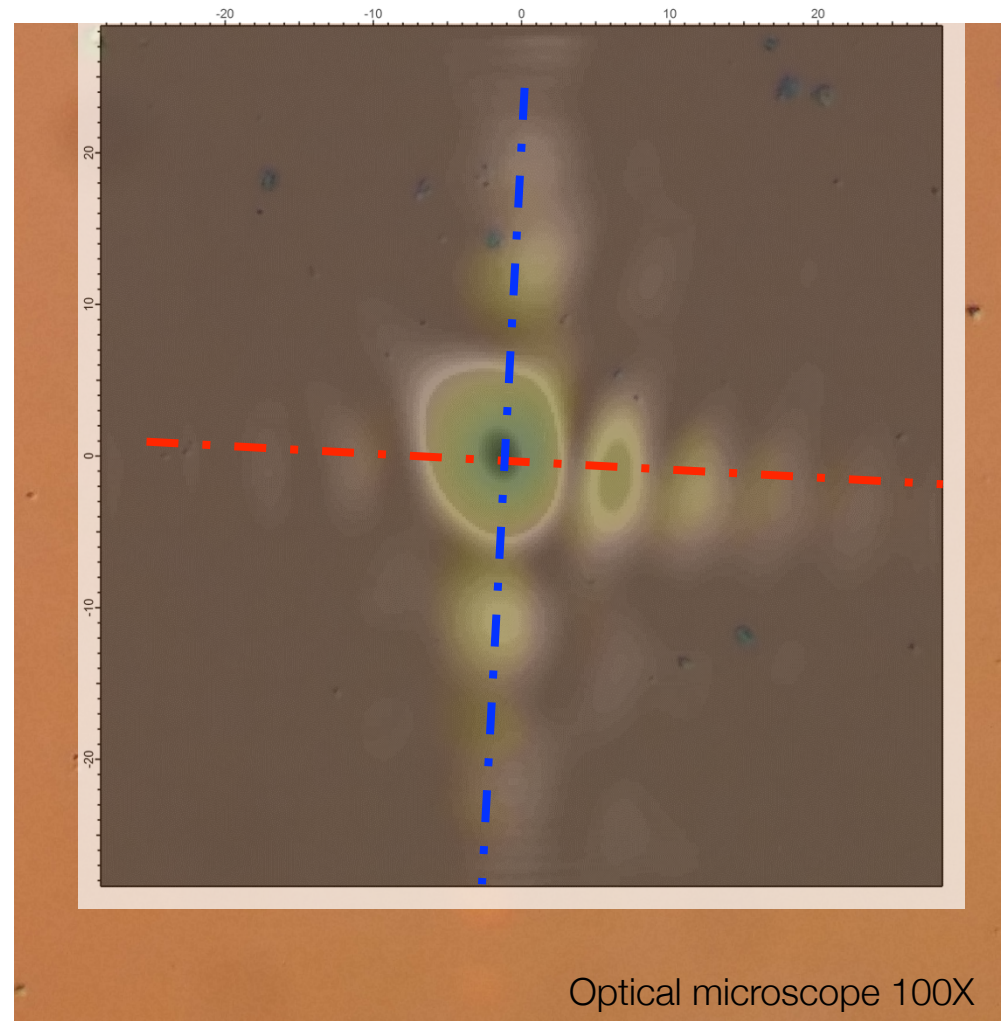


Simulations

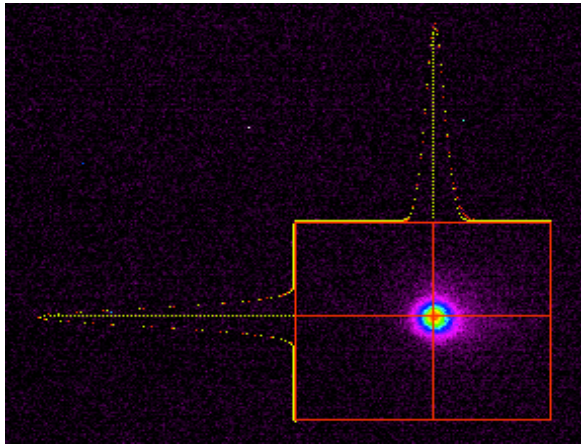


- (1) L. Raimondi, D. Spiga, SPIE Proc., 8147 (2011)
- (2) L. Raimondi et al., NIM A, 710, 131 (2013)

### PMMA ablation imprint



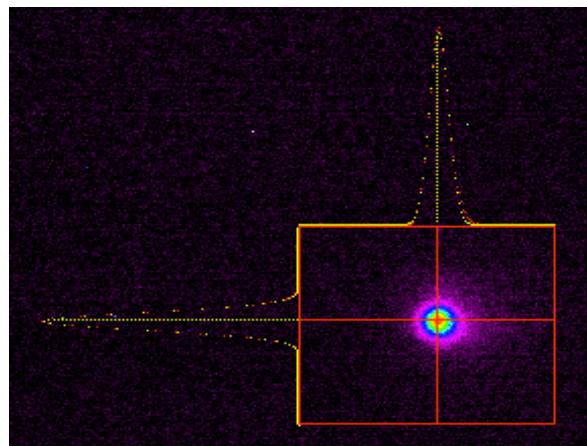
**Good agreement** between in-house  
reconstruction, PMMA, simulations



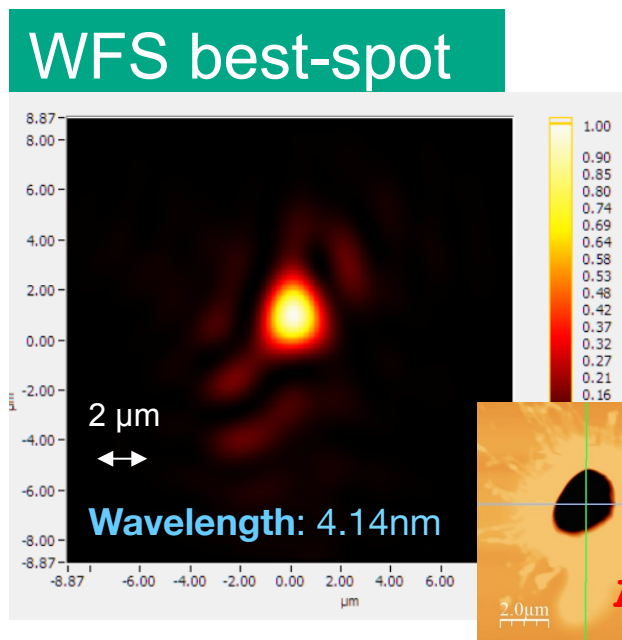
Focal spot of the **ellipsoidal mirror**  
( $10 \times 10 \mu\text{m}^2$  FWHM) with FEL-1

Best focus routinely achieved with the ellipsoidal mirror on FEL-1 (even though the mirror is optimized for FEL-2 (shorter entrance arm wrt FEL-1))



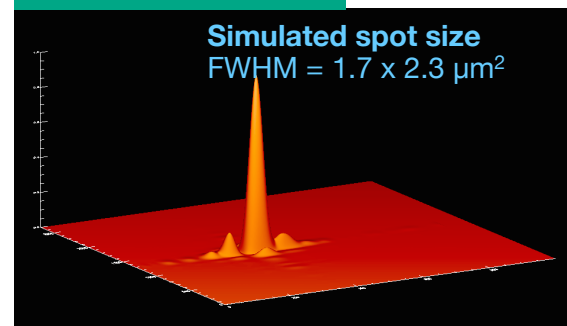


Focal spot of the **ellipsoidal mirror**  
( $10 \times 10 \mu\text{m}^2$  FWHM) with FEL-1

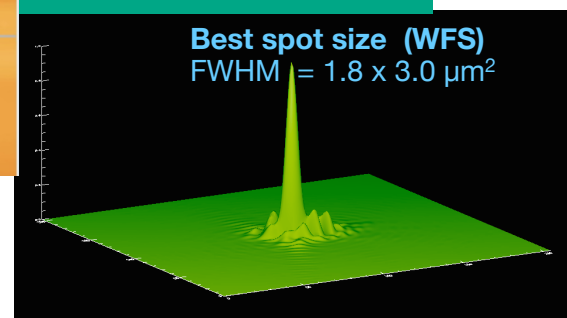


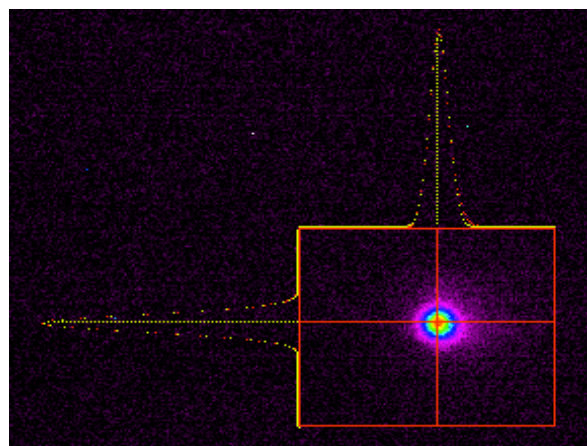
Focal spot sizes as low as **1.8  $\mu\text{m}$**   
(FWHM) with FEL-2 ( $\sim 4$  nm)

Simulated spot



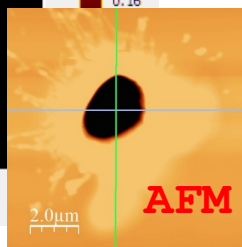
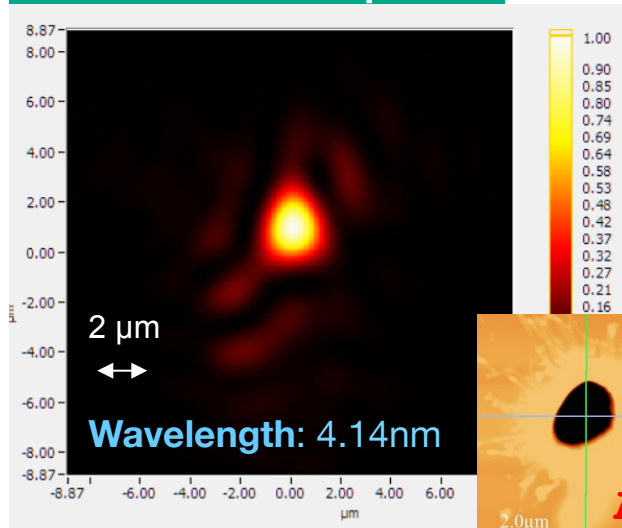
Measured spot (best)



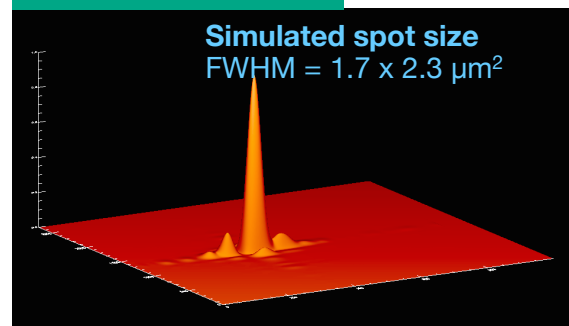


Focal spot of the **ellipsoidal mirror** ( $10 \times 10 \mu\text{m}^2$  FWHM)

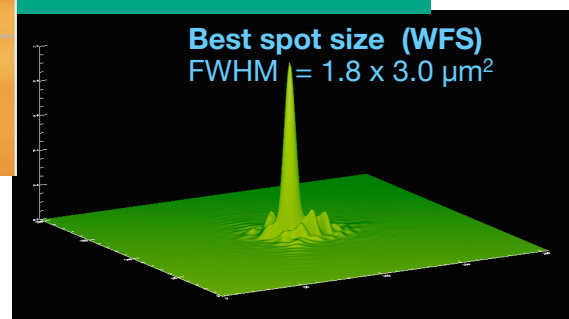
### WFS best-spot



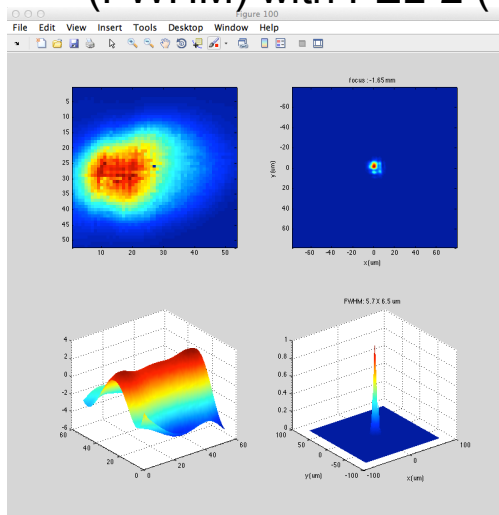
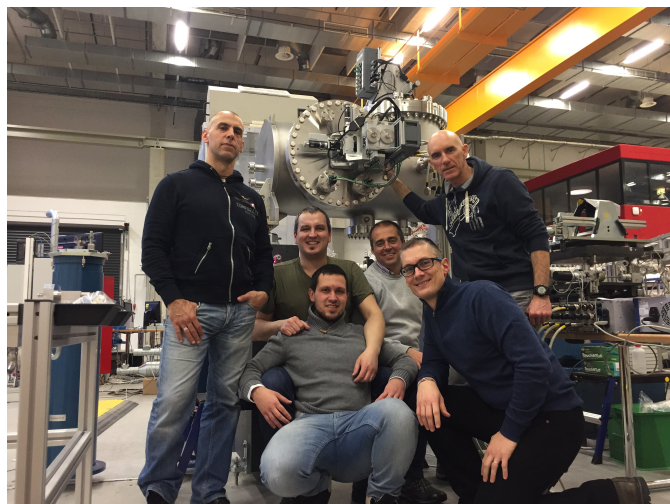
### Simulated spot



### Measured spot (best)

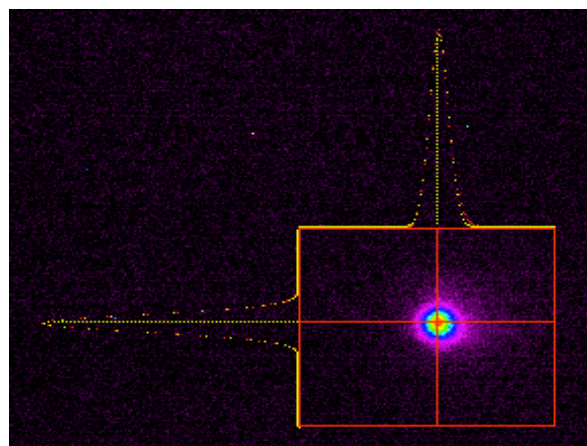


Focal spot sizes as low as  **$1.8 \mu\text{m}$**  (FWHM) with FEL-2 ( $\sim 4 \text{ nm}$ )



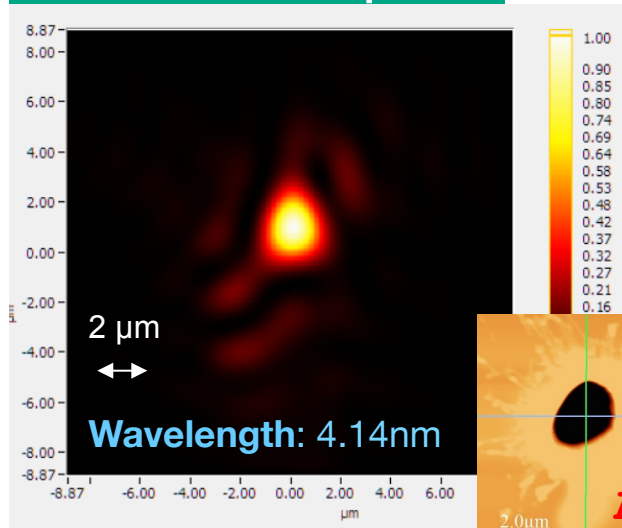
### Installation of a KAOS at FLASH2 (March 2017)

After very little time  $\rightarrow 5.7 \times 6.5 \mu\text{m}^2$  (close to target value and obtained with not optimized FEL)



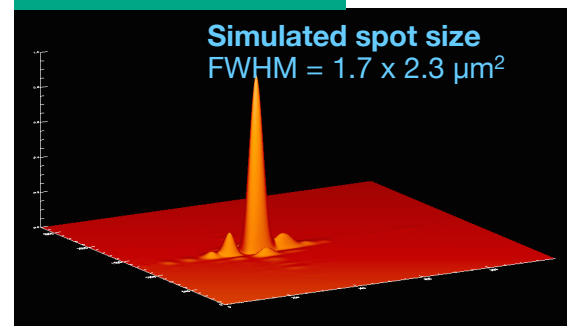
Focal spot of the **ellipsoidal mirror** ( $10 \times 10 \mu\text{m}^2$  FWHM)

### WFS best-spot

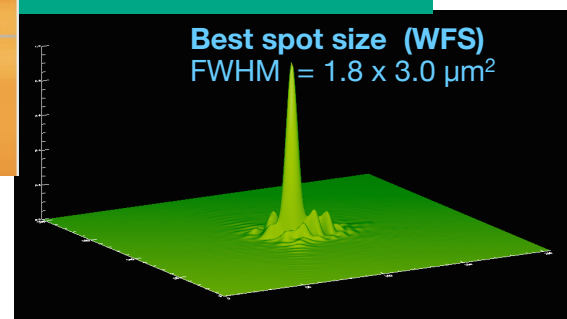


Focal spot sizes as low as  **$1.8 \mu\text{m}$**  (FWHM) with FEL-2 ( $\sim 4 \text{ nm}$ )

### Simulated spot



### Measured spot (best)



### FERMI experience:

The **focusing optimization** and consequent **spot size characterization** is fundamental for experiments and must be pursued by means of non-invasive and online diagnostics → the wavefront sensor is the best, so far.

In order to fulfill user diverse and often exotic requests, the **active optics systems** (like KAOS, for instance) seem to represent the best solution.

With not optimized FEL



In experiments where dynamic processes are expected to occur during FEL exposure the **FEL pulse profile** must be measured with femtosecond accuracy on a single-shot basis. Moreover, determination of **time-arrival** is mandatory for proper synchronization in pump-probe experiments.

- THz streaking

Good if jitter is not too large

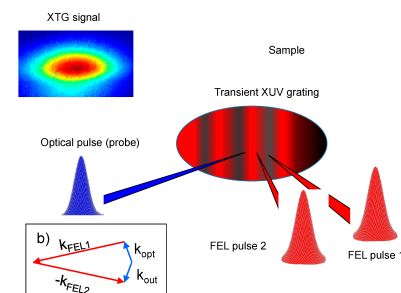
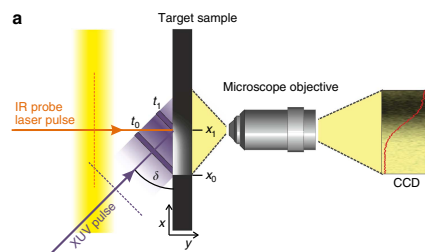
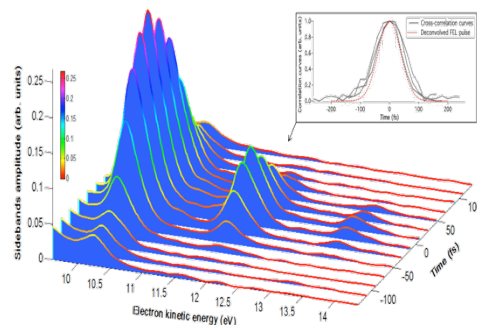
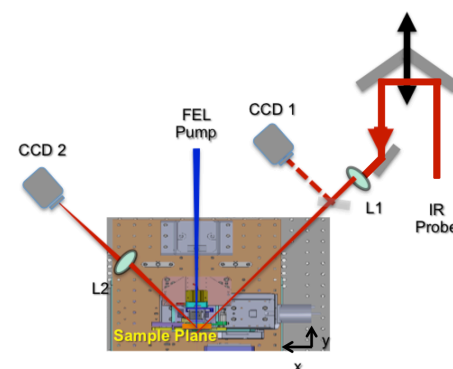
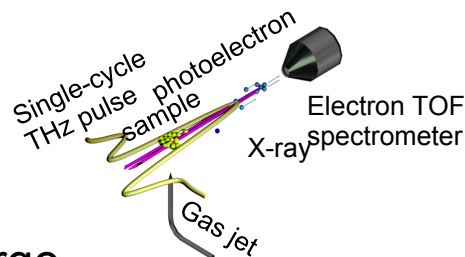
- Transmission/reflectivity spatial and spectral encoding

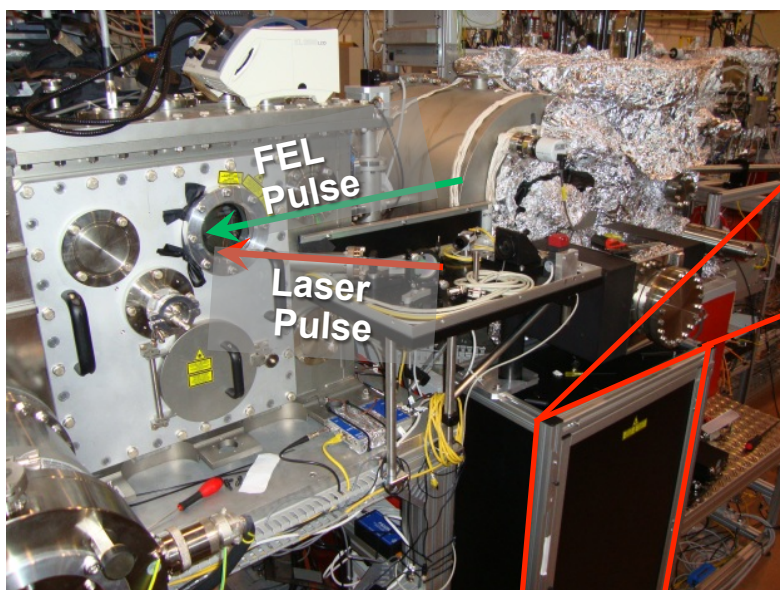
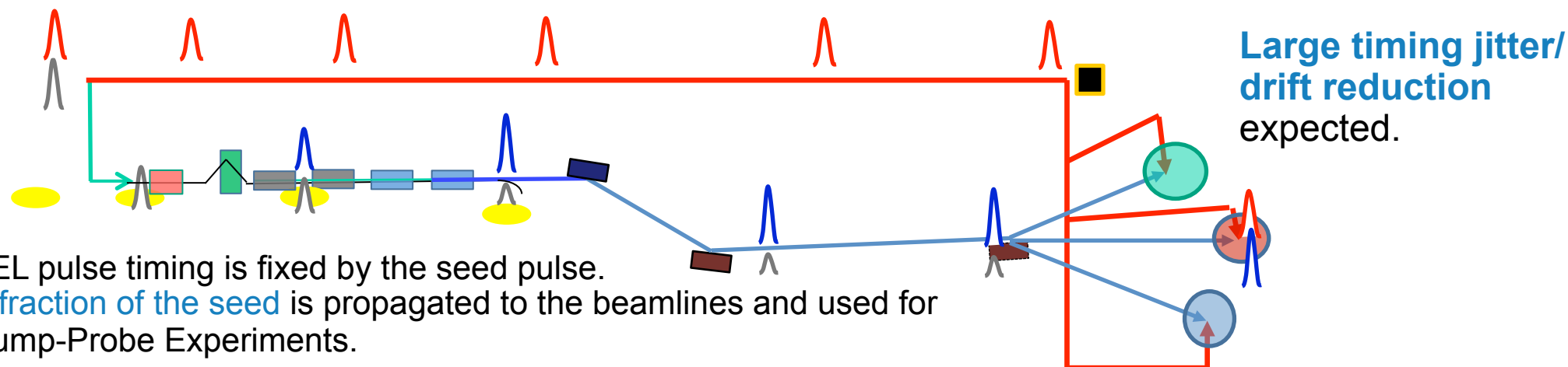
Information only about arrival time

- Sidebands in electronic spectra

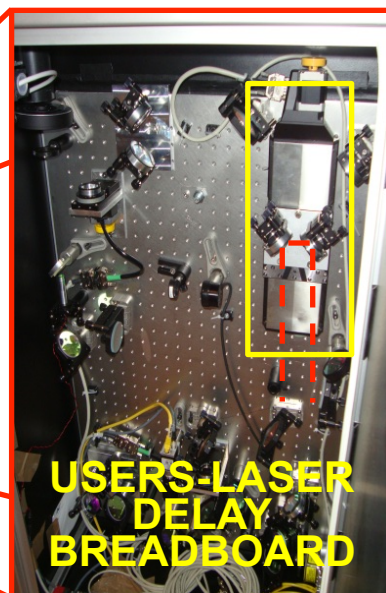
- Plasma gating

- Transient Grating-based measurements (see F. Bencivenga tomorrow)

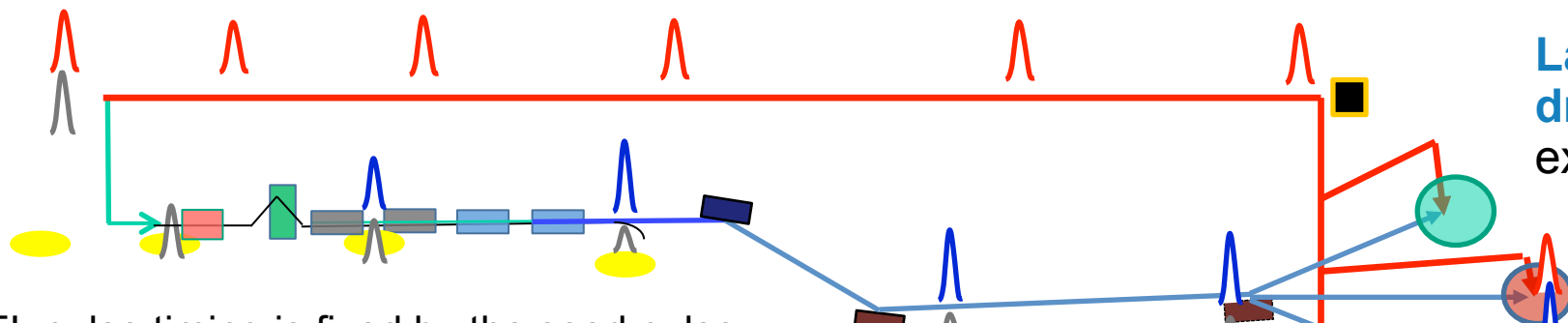




Since Feb-2013 DiProI end station equipped with external user laser

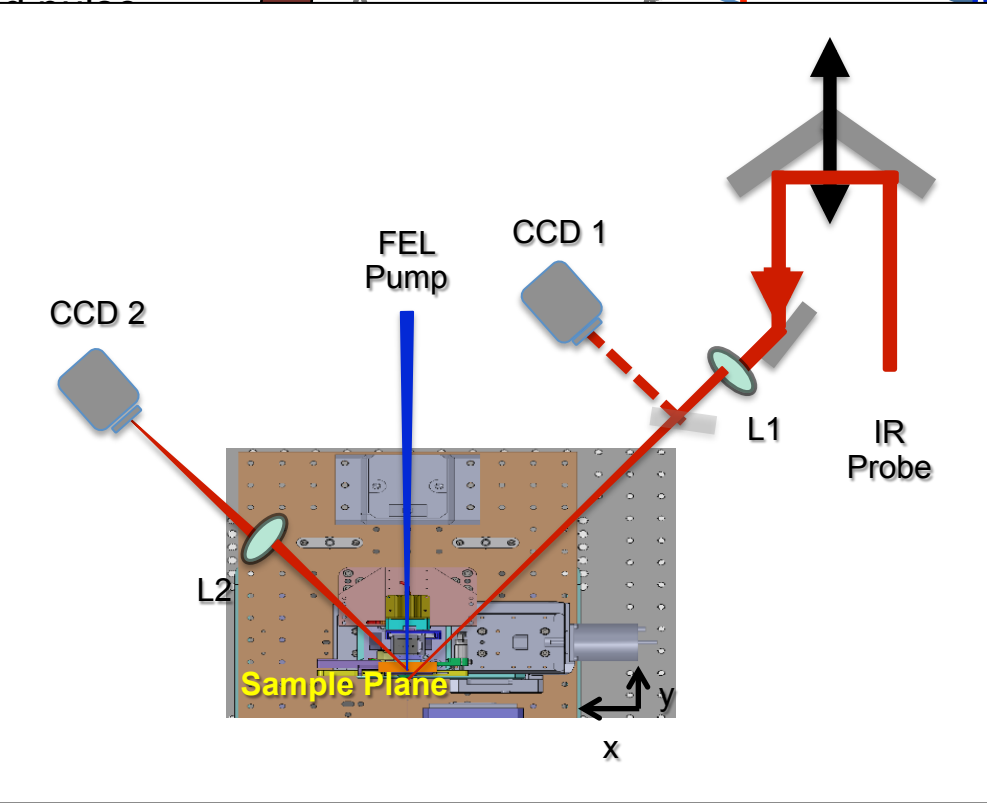
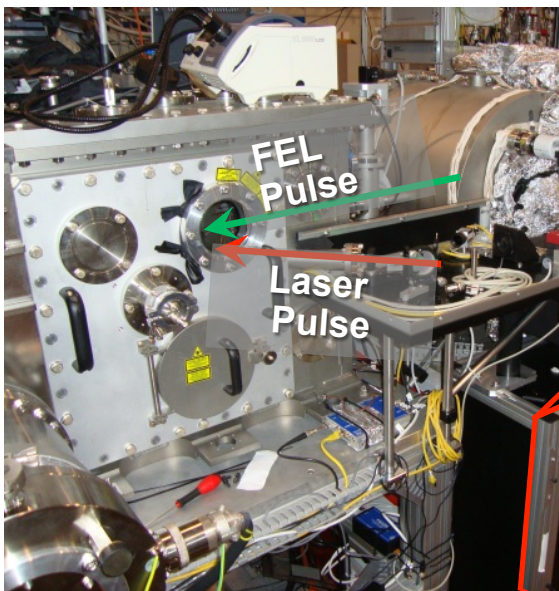


- Two pass optical delay line  $\pm 600\text{ps}$
- Automatic attenuator plate and vertical horizontal polarizer
- Laser shot-by-shot Intensity monitor
- Pulse selector shutter



Large timing jitter/  
drift reduction  
expected.

FEL pulse timing is fixed by the seed  
A fraction of the seed is propagated  
Pump-Probe Experiments.



cal delay line  $\pm 600\text{ps}$

nuator plate and  
ntal polarizer

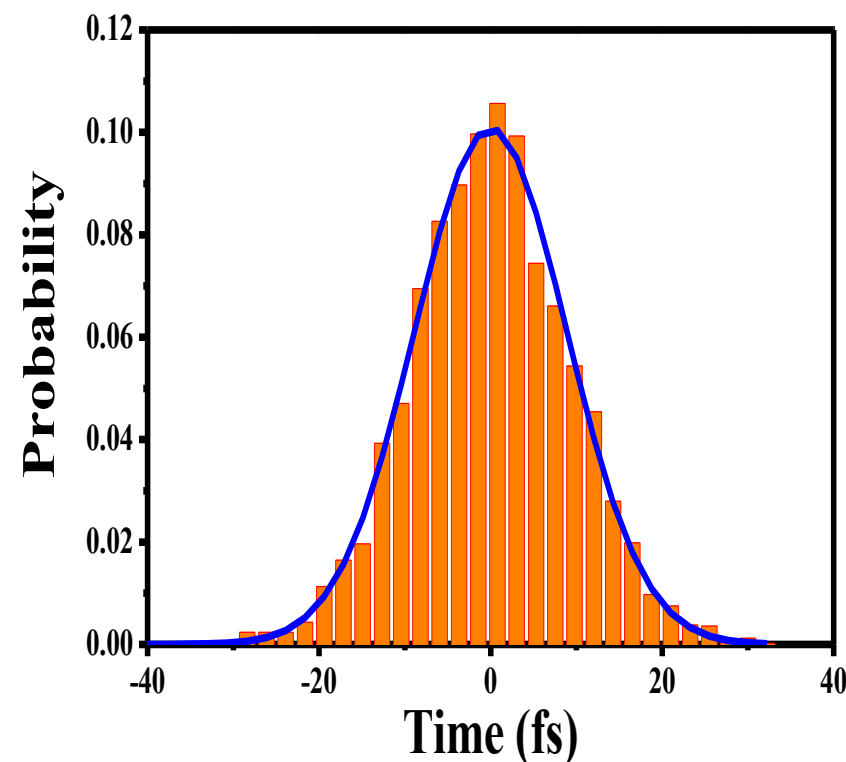
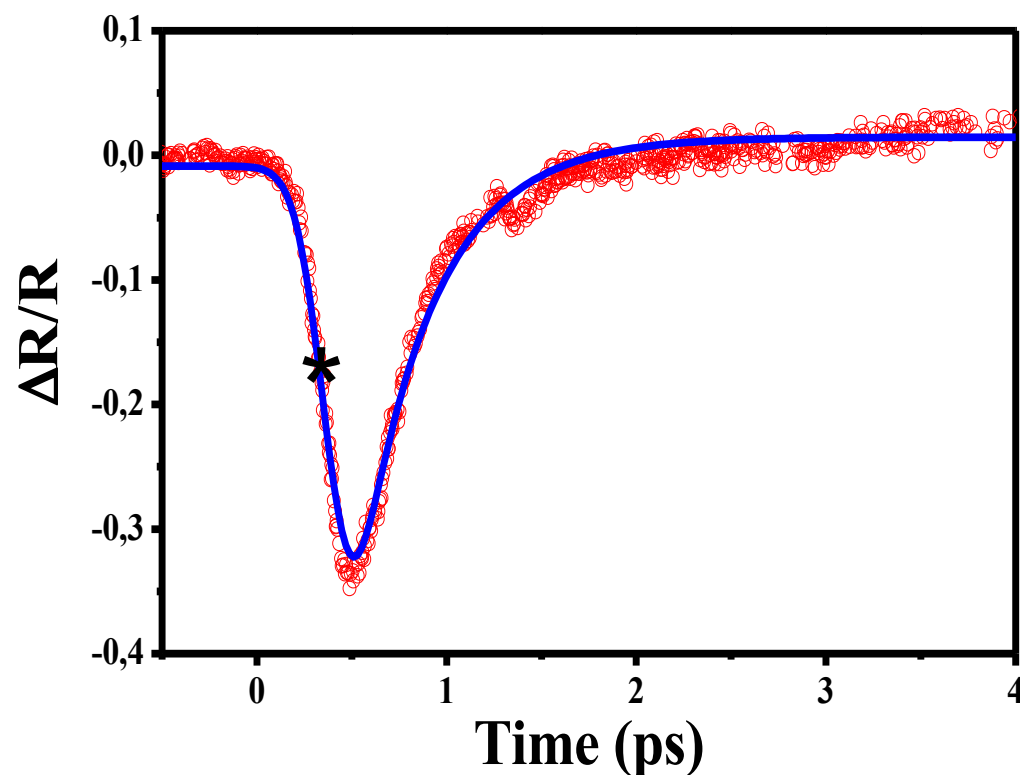
shot Intensity

shutter

Since Feb-2013 DiProl end st  
equipped with external user laser

**BREADBOARD**





M.Danailov, et al., Optics Express 22, 12869 (2014)

Arrival time jitter FEL-IR laser **< 6±2 fs (RMS)** → 2μm over 100m-path length !!!  
(Measured at the ½ drop point of the reflectivity curve)

Long term (~1 day) stability time zero between FEL and IR laser **~70 – 60 fs**.

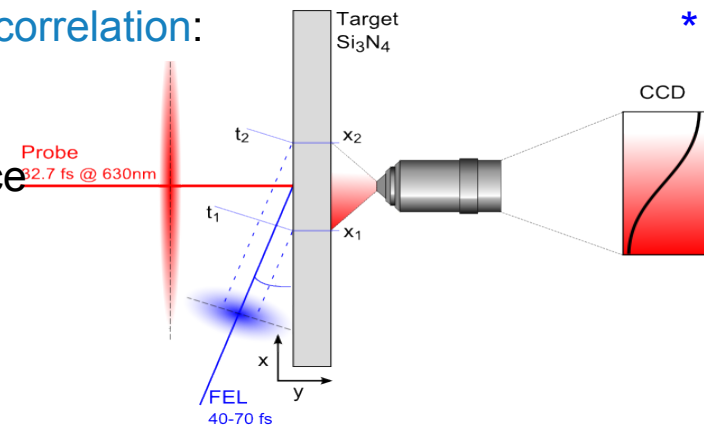
Recent result @DiProi: 2.2fs RMS jitter between a NOPA Pumped by the IR seed and FEL

**Two cross-correlation methods** have been implemented and used for **measuring the FEL pulse length**.

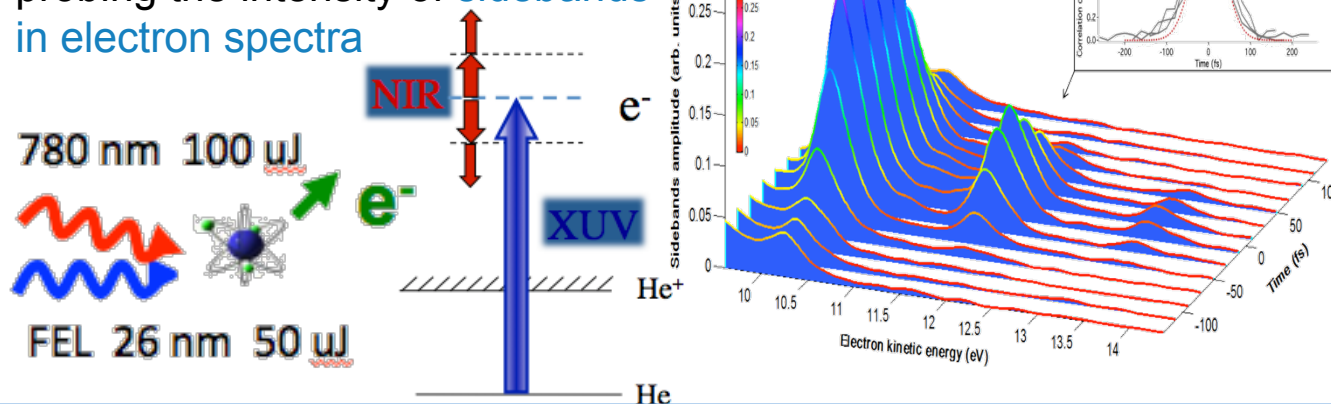
In both cases FEL pulse length has been studied as a function of seed laser parameters and FEL wavelength.

**Solid state cross correlation:**

temporally & spatially encode FEL on the surface of a  $\text{Si}_3\text{N}_4$  target probed with an ultrashort laser pulse



Cross correlation measurement probing the intensity of **sidebands** in electron spectra



$\lambda_{seed}$ (nm)	$\lambda_{FEL}$ (nm)	$\tau_{seed}$ (fs)	$\tau_{FEL}$ (fs)
257.8	25.78	140	$61.5 \pm 3$
261.1	23.74	140	$63 \pm 4$
261.1	20.08	140	$74 \pm 3$
261.7	37.38	112.5	$52 \pm 8$
261.7	26.17	112.5	$53 \pm 3$
261.7	26.17	157.5	$72 \pm 6$
261.7	18.69	112.5	$42 \pm 6$

**Expected FEL pulse shortening at higher harmonics (shorter wavelength) has been confirmed by measurements.**

P. Finetti et al. Phys. Rev. X 7, 021043 (2017)

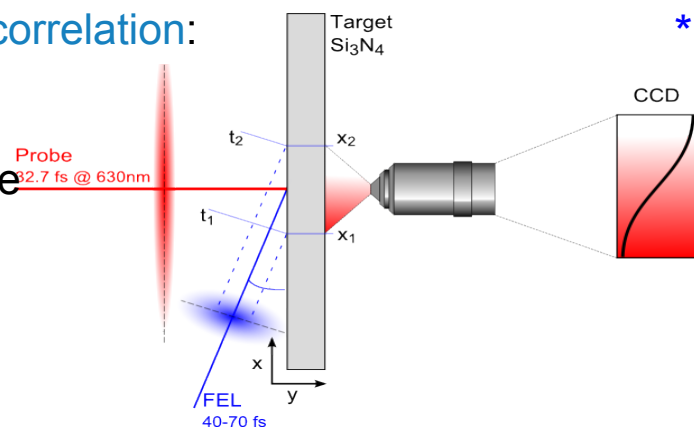
\* In collaboration with F. Tavella team

\*\* In collaboration with C. Callegari and LDM team

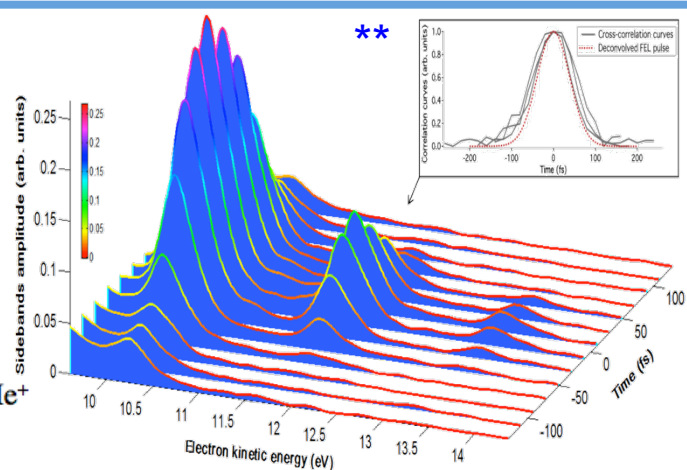
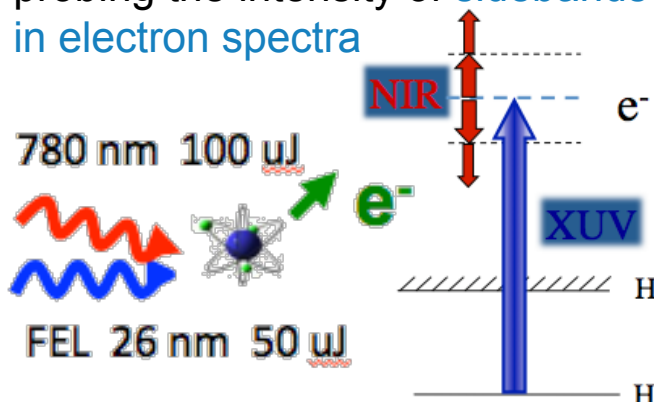
**Two cross-correlation methods** have been implemented and used for **measuring the FEL pulse length**.

In both cases FEL pulse length has been studied as a function of seed laser parameters and FEL wavelength.

**Solid state cross correlation:** temporally & spatially encode FEL on the surface of a  $\text{Si}_3\text{N}_4$  target probed with an ultrashort laser pulse



Cross correlation measurement probing the intensity of **sidebands** in electron spectra



$\lambda_{seed}$ (nm)	$\lambda_{FEL}$ (nm)	$\tau_{seed}$ (fs)	$\tau_{FEL}$ (fs)
257.8	25.78	140	$61.5 \pm 3$
261.1	23.74	140	$63 \pm 4$
261.1	20.08	140	$74 \pm 3$
261.7	37.38	112.5	$52 \pm 8$
261.7	26.17	112.5	$53 \pm 3$
261.7	26.17	157.5	$72 \pm 6$
261.7	18.69	112.5	$42 \pm 6$

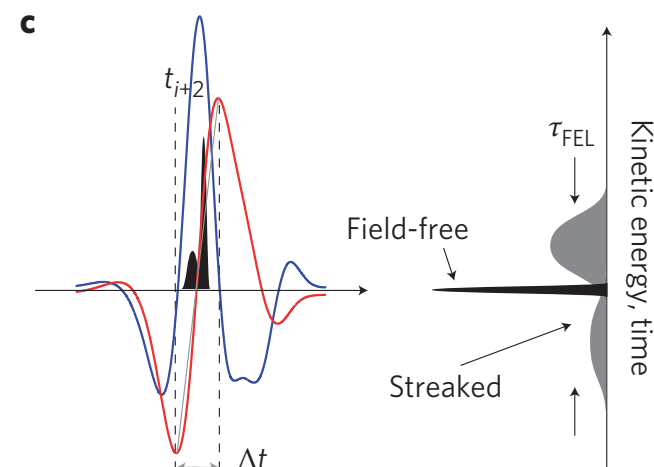
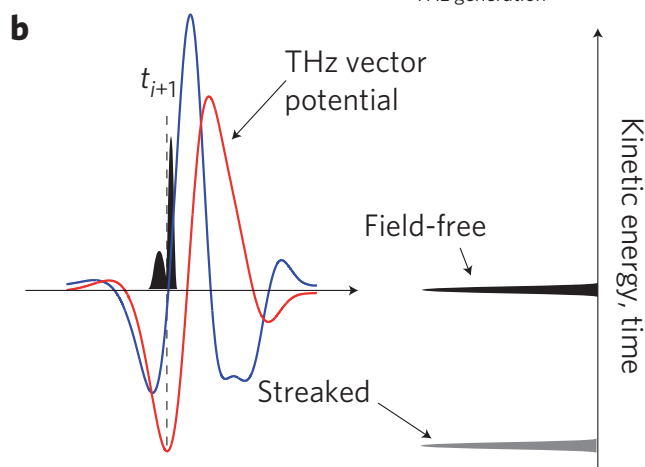
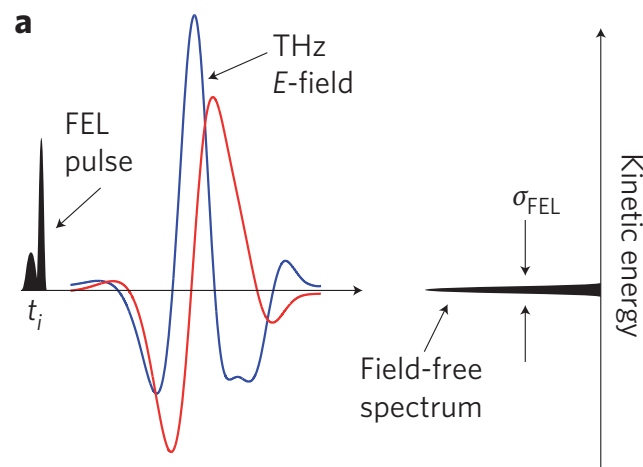
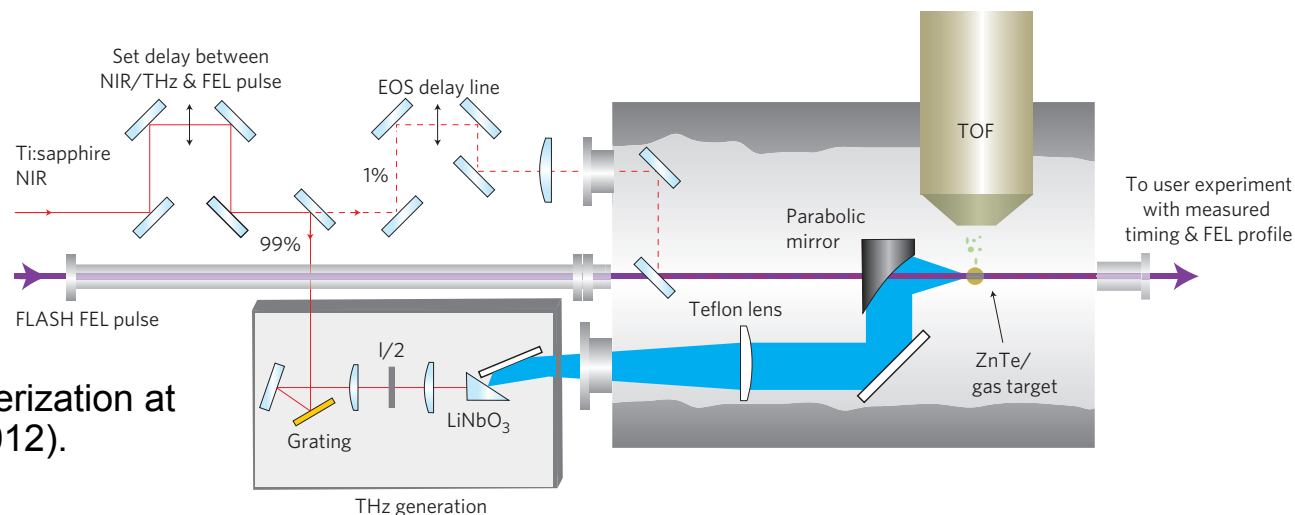
### FERMI experience:

The pulse length/time profile/arrival time determination can still be seen as an **experiment on its own**. The cross correlation-based techniques cannot serve as online, non invasive diagnostics. A different scheme should be employed.



Full temporal characterization  
using independent optical laser-  
driven single-cycle THz pulses for  
fs time-resolved photoelectron  
spectroscopy

Grguraš, I. *et al.* Ultrafast X-ray pulse characterization at  
free-electron lasers. *Nat. Phot.* 6, 852-857 (2012).



Transparent inline geometry  
XUV – HXR

10 – 100 fs pulses

Using standard laser technology

Not requiring dedicated accelerator infrastructure

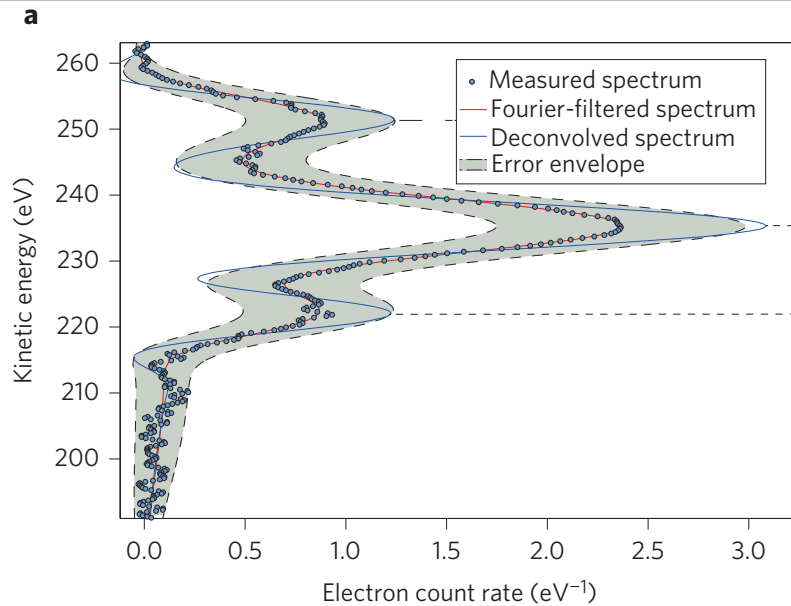
# PULSE LENGTH / ARRIVAL TIME

## Optical laser-driven THz streaking

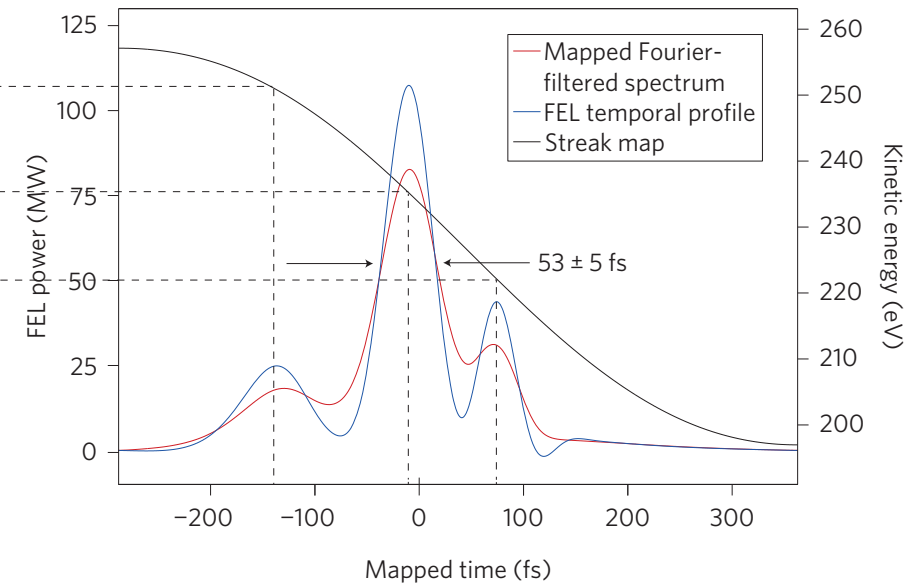
Full t  
using  
drive  
fs tim  
spec

Grgura  
free-e

**a**



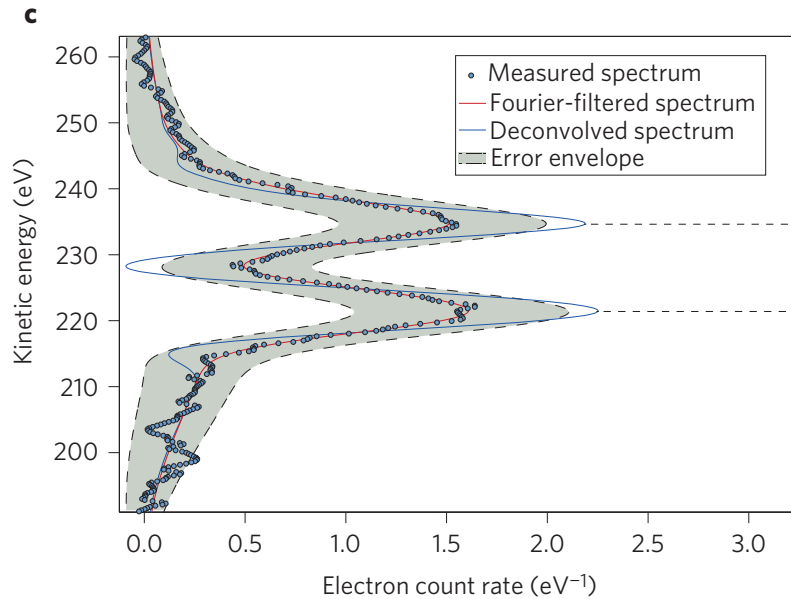
**b**



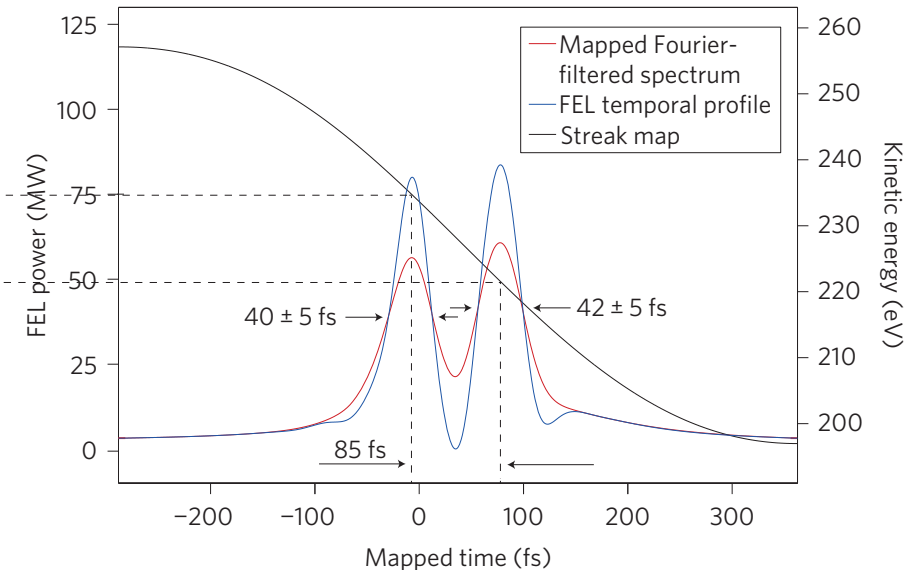
To user experiment  
with measured  
timing & FEL profile

Kinetic energy, time  
 $\tau_{\text{FEL}}$

**c**



**d**

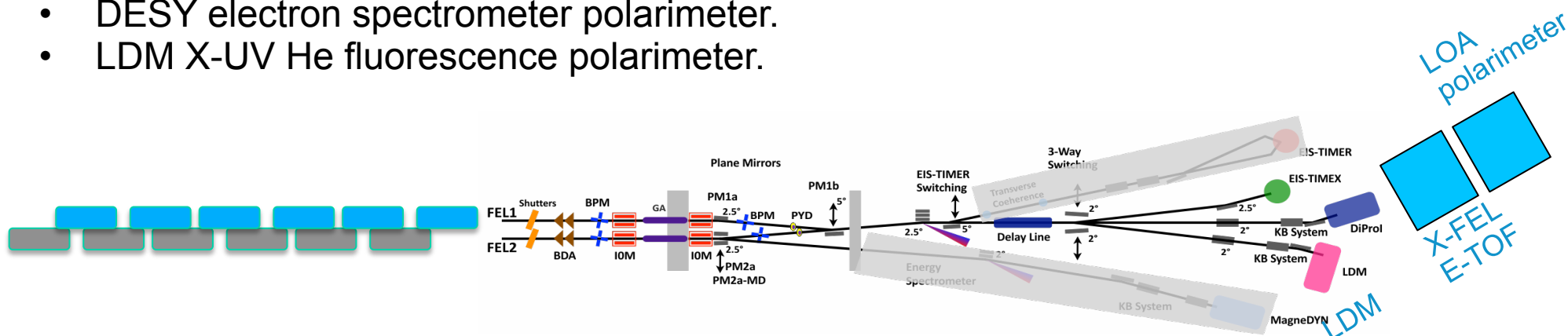


Tra  
XU  
10  
Usi  
Not

### APPLE-II undulators in the final radiator ensure **polarization control**

Three different setups for characterization of the FERMI FEL polarization (coord. E.Allaria):

- LOA optical UV polarimeter.
- DESY electron spectrometer polarimeter.
- LDM X-UV He fluorescence polarimeter.



### Characterization of the FEL polarization produced by APPLE-2 undulators at 32nm, 26nm, 43nm, 53nm

- Horizontal/Vertical polarization.
- Circular polarization.

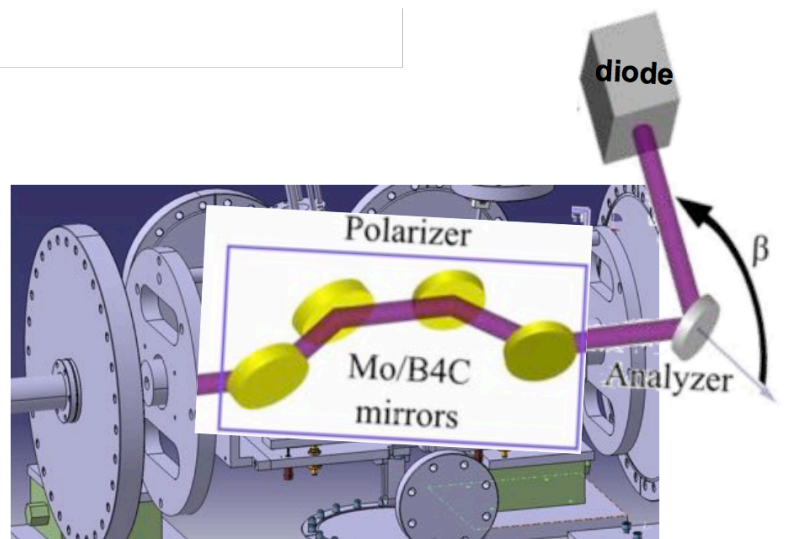
### Studies of cross-polarized schemes to control the polarization

- Circular right and left for generating linear polarization.
- Linear vertical and horizontal for generating circular polarization.



# POLARIZATION MEASUREMENT

## EUV and Visible light polarimeters

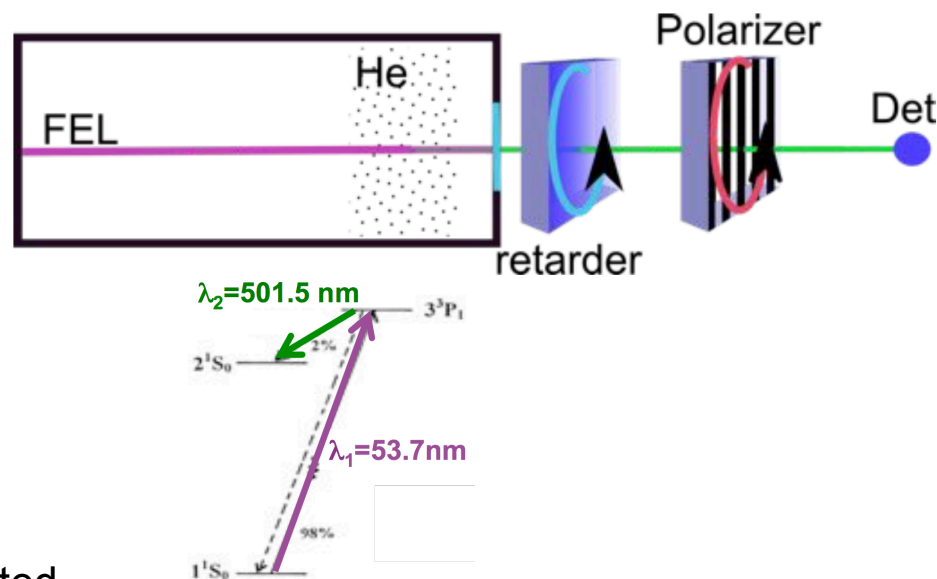


**Optical polarimeter for EUV sources (LOA):** 4 coated grazing incidence mirrors used as phase retarder for  $s$  and  $p$  field components and a  $45^\circ$  mirror used as a polarizer.

Setup installed at FERMI: suitable for characterizing 26nm and 32nm with circular and vertical polarizations.

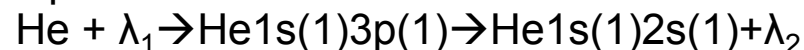
Proper fit of the measured detector signal as a function of the detector angle  $\beta \rightarrow$  FEL polarization state

E. Allaria et al. Phys. Rev. X **4**, 041040 (2014)

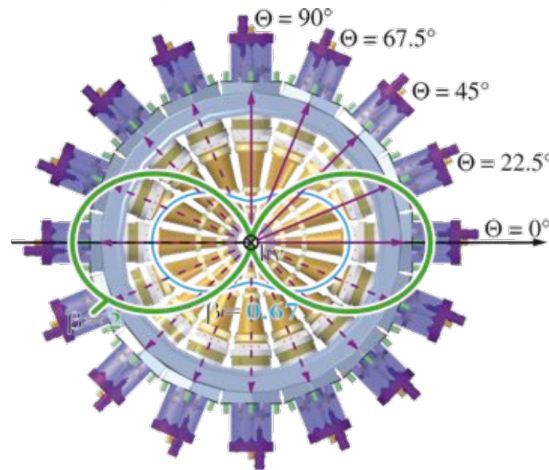
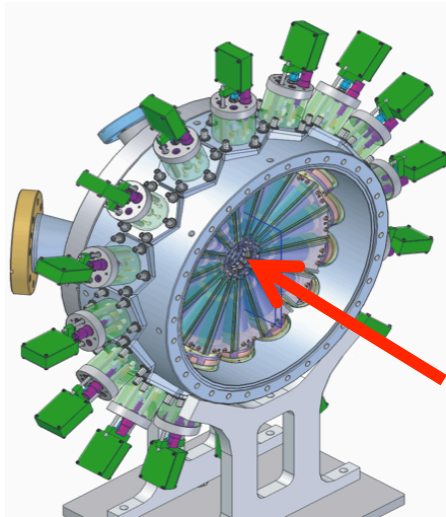


Measuring the polarization of **fluorescence light emitted in the visible range** following suitable X-UV excitations  $\rightarrow$  FEL polarization state

Optical transitions selected:



Polarization measured in the visible with standard optical methods using a retarder ( $\lambda/4$ ) and a polarizer. Acquisition are done by scanning the polarizer angle for various values of the retarder angle.



A **single shot polarimeter** based on angle resolving electron spectrometer (J.Viefhaus' group at DESY)

Theory predicts specific electron distributions over the 16 detectors depending on the used gas and FEL polarization.

### Diagnostics

- Versatile online beam diagnostics unit
- Used at PETRA III, FERMI, LCLS, ...
- Feasible as a (X)FEL diagnostic
- Polarization characterization on a shot-to-shot

### Detection scheme

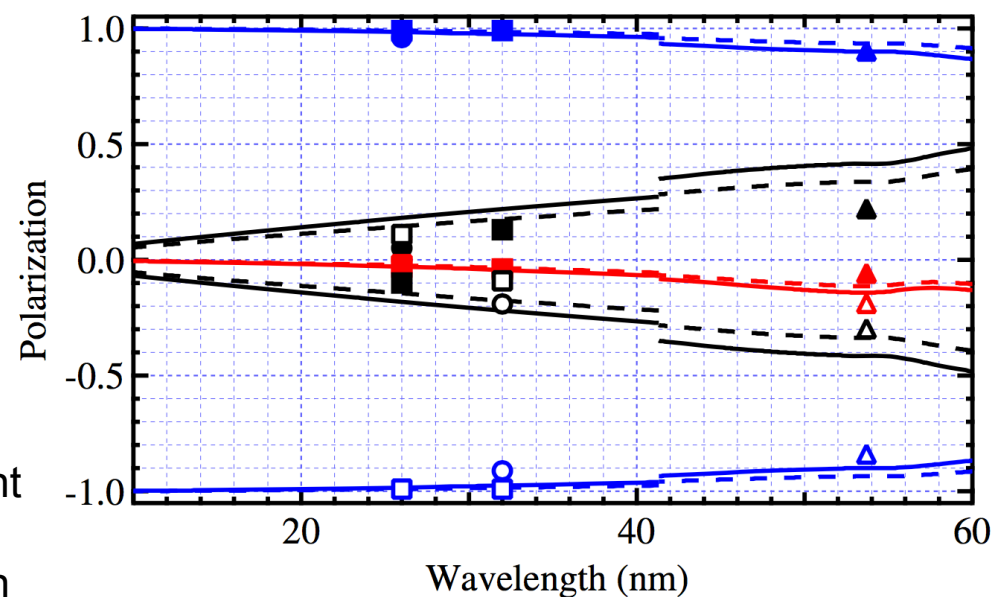
- Single-shot spectra → High detection efficiency  $\sim 4\%$  of  $4\pi$
- Energy resolution → Resolution up to  $10^{-3}$
- Angular resolution → 16 spectrometers  $22.5^\circ$
- Energy range → 0.02-25 keV (for European XFEL)

# POLARIZATION MEASUREMENT Results

DESY					
$\lambda$	Polarization	S1	S2	S3	Pol
26 nm	Vertical	-0.97	0.01	0.2	<b>0.97</b>
26 nm	Circ Right	-0.02	0.10	0.99	<b>0.99</b>
32 nm	Vertical	-0.91	-0.04	0.40	<b>0.97</b>
32 nm	Circ Right	-0.04	-0.13	0.99	<b>0.99</b>

LOA					
$\lambda$	Polarization	S1	S2	S3	Pol
26 nm	Vertical	-0.95	0	0.07	<b>0.95</b>
26 nm	Circular R	0	0.05	0.96	<b>0.96</b>
32 nm	Vertical	-0.96	0	0.06	<b>0.96</b>
32 nm	Circ Right	-0.05	-0.19	0.90	<b>0.92</b>

LDM					
$\lambda$	Polarization	S1	S2	S3	Pol
52 nm	Horizontal	0.92	0.11	0	<b>0.92</b>
52 nm	Circ Right	-0.07	0.21	0.89	<b>0.91</b>
52 nm	Circ Left	-0.20	-0.31	-0.85	<b>0.93</b>



Measurements of the degree of polarization with different polarimeters has shown a **good control of the polarization\*** allowing switching from linear to circular in the whole spectral range of operation.

E. Allaria et al. Phys. Rev. X **4**, 041040 (2014)

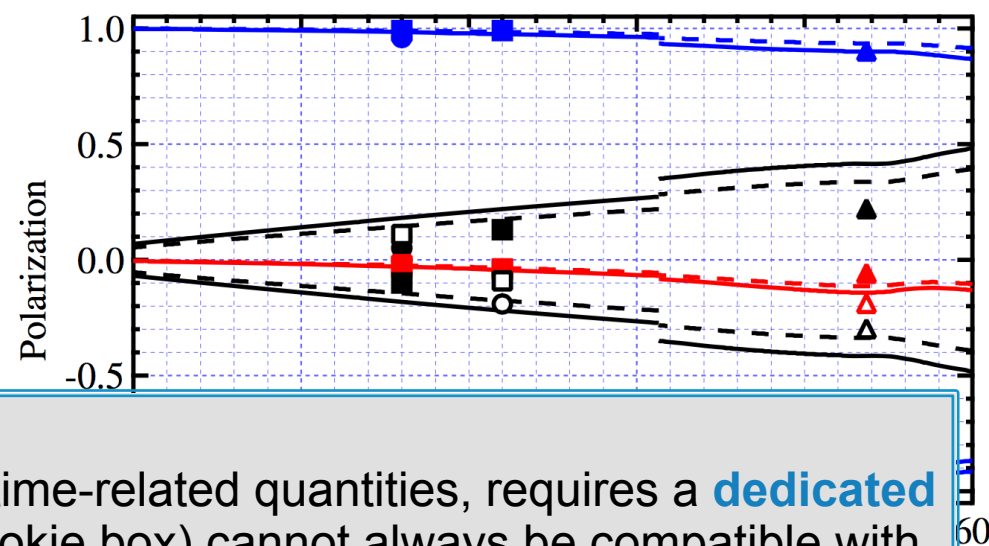


# POLARIZATION MEASUREMENT Results

DESY					
$\lambda$	Polarization	S1	S2	S3	Pol
26 nm	Vertical	-0.97	0.01	0.2	<b>0.97</b>
26 nm	Circ Right	-0.02	0.10	0.99	<b>0.99</b>
32 nm	Vertical	-0.91	-0.04	0.40	<b>0.97</b>
32 nm	Circ Right	-0.04	-0.13	0.99	<b>0.99</b>

LOA					
$\lambda$	Polarization	S1	S2	S3	Pol
26 nm	Vertical	-0.95	0	0.07	<b>0.95</b>
26 nm	Circular R	0	0.05	0.96	<b>0.96</b>
32 nm	Vertical	-0.96	0	0.06	<b>0.96</b>
32 nm	Circ Right	-0.05	-0.19	0.90	<b>0.92</b>

LDM					
$\lambda$	Polarization	S1	S2	S3	Pol
52 nm	Horizontal	0.92	0.11	0	<b>0.92</b>
52 nm	Circ Right	-0.07	0.21	0.89	<b>0.91</b>
52 nm	Circ Left	-0.20	-0.31	-0.85	<b>0.93</b>



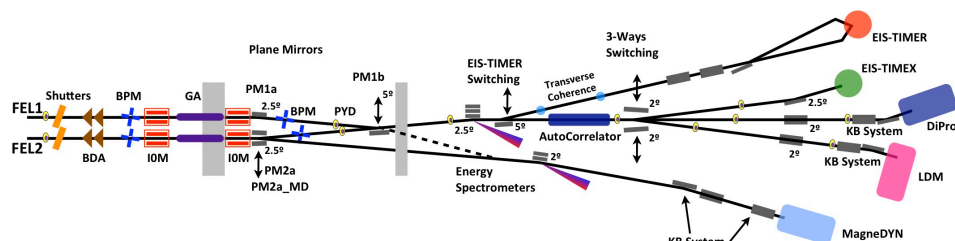
## FERMI experience:

The polarization determination, similarly to the time-related quantities, requires a **dedicated experiment** or at least (as in the case of the cookie box) cannot always be compatible with normal user operation at a facility.

E. Allaria et al. Phys. Rev. X **4**, 041040 (2014)

### Photon diagnostics

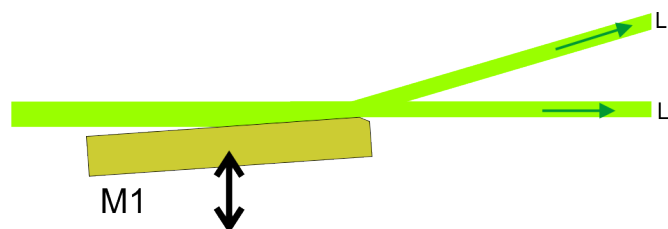
**multi-diagnostics** along the transport:  
intensity (different types), spectrum,  
pulse length, time arrival, spot size, ...



### Endstations operation

**multi-endstation**

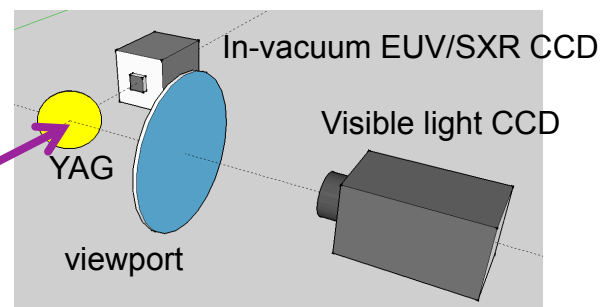
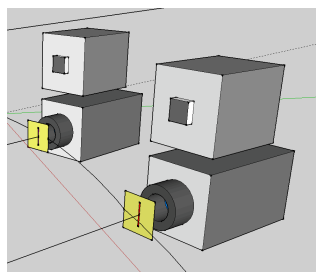
(WF splitting) → soon at FERMI



### Energy spectrometer

- **multi-color** mode  
(2 independent detection units)
- **multi-detectors**

(optimizing efficiency to  $\lambda$ ) → soon at FERMI

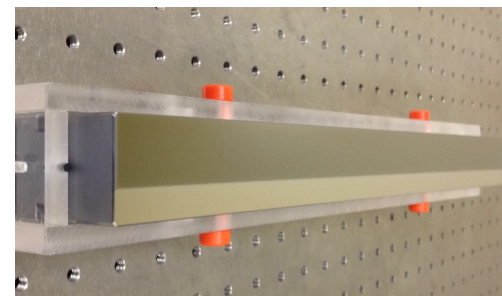


### Optics

**multi-coatings**/stripes (to optimize the reflectivity)

→ soon/already at FERMI

[particularly challenging for active optics systems]





A large group of people, approximately 100-150 individuals, are posed for a group photograph in a large, open hall. The hall features tiered seating in the background, suggesting an auditorium or lecture hall. The people are arranged in several rows, filling the central area of the room. The lighting is bright, and the overall atmosphere is formal yet celebratory.

# THANK YOU

Allaria E., Bencivenga F., Callegari C., Capotondi F., Castronovo D., Cinquegrana P., Craievich P., Cudin I., Danailov M.B., De Monte R., Demidovich A., D'Auria G., Dal Forno M., De Ninno G., Di Mitri S., Diviacco B., Fabris A., Fabris R., Fava C., Fawley W.M., Ferianis M., Ferrari E., Finetti P., Froehlich L., Furlan Radivo P., Gaio G., Gauthier D., Gerusina S., Giannessi L., Gobessi R., Ivanov R., Kiskinova M., Kurdi G., Loda G., Lonza M., Mahne N., Mahieu B., Manfredda M., Masciovecchio C., Mazzucco E., Predonzani M., Principi E., Nikolov I., Parmigiani F., Penco G., Plekan O., Prince K.C., Raimondi L., Rossi F., Roussel E., Rumiz L., Serpico C., Sigalotti P., Scafuri C., Spampinati S., Spezzani C., Sturari L., Svandrlik M., Svetina C., Trovò M., Vascotto A., Veronese M., Visintini R., Zangrando D., and MANY MORE including users, collaborators, visitors, administrative people...